Monthly Notices of the ROYAL ASTRONOMICAL SOCIETY **MNRAS Advance Access published November 26, 2013**

MNRAS (2013) doi:10.1093/mnras/stt1975

On the nature of the 'hostless' short GRBs

R. L. Tunnicliffe,[1]★ A. J. Levan,[1] N. R. Tanvir,[2] A. Rowlinson,[3] D. A. Perley,[4] J. S. Bloom,[4] S. B. Cenko,[4] P. T. O'Brien,[2] B. E. Cobb,[4] K. Wiersema,[2] D. Malesani,[5] A. de Ugarte Postigo,[5] J. Hjorth,[5] J. P. U. Fynbo[5] and P. Jakobsson[6]

[1]*Department of Physics, University of Warwick, Coventry CV4 7AL, UK*
[2]*Department of Physics and Astronomy, University of Leicester, Leicester LE1 7RH, UK*
[3]*Astronomical Institute, University of Amsterdam, Science Park 904, NL-1098 XH Amsterdam, the Netherlands*
[4]*Department of Astronomy, University of California, Berkeley, CA 94720-3411, USA*
[5]*Dark Cosmology Centre, Niels Bohr Institute, University of Copenhagen, DK-2100 Copenhagen, Denmark*
[6]*Centre for Astrophysics and Cosmology, Science Institute, University of Iceland, Dunhaga 5, IS-107 Reykjavik, Iceland*

Accepted 2013 October 14. Received 2013 October 12; in original form 2012 August 25

ABSTRACT

A significant proportion (∼30 per cent) of the short-duration gamma-ray bursts (SGRBs) localized by *Swift* have no detected host galaxy coincident with the burst location to deep limits, and also no high-likelihood association with proximate galaxies on the sky. These SGRBs may represent a population at moderately high redshifts ($z \gtrsim 1$), for which the hosts are faint, or a population where the progenitor has been kicked far from its host or is sited in an outlying globular cluster. We consider the afterglow and host observations of three 'hostless' bursts (GRBs 090305A, 091109B and 111020A), coupled with a new observational diagnostic to aid the association of SGRBs with putative host galaxies to investigate this issue. Considering the well localized SGRB sample, 7/25 SGRBs can be classified as 'hostless' by our diagnostic. Statistically, however, the proximity of these seven SGRBs to nearby galaxies is higher than is seen for random positions on the sky. This suggests that the majority of 'hostless' SGRBs have likely been kicked from proximate galaxies at moderate redshift. Though this result still suggests only a small proportion of SGRBs will be within the Advanced Laser Interferometer Gravitational Wave Observatory horizon for neutron star–neutron star (NS) or neutron star–black hole (BH) inspiral detection ($z \sim 0.1$), in the particular case of GRB 111020A a plausible host candidate is at $z = 0.02$.

Key words: techniques: photometric – gamma-ray burst: individual: 090305A – gamma-ray burst: individual: 091109B – gamma-ray burst: individual: 110112A – gamma-ray burst: individual: 111020A – stars: neutron.

1 INTRODUCTION

Short-duration gamma-ray bursts (SGRBs)[1] reside in different environments from their long GRB counterparts (LGRBs). While LGRBs are usually found in the brightest regions of star-forming host galaxies (Bloom, Kulkarni & Djorgovski 2002; Fruchter et al. 2006), SGRBs often appear in galaxies with established older populations with a handful linked strongly to elliptical (Ell) galaxy hosts (Berger et al. 2005; Gehrels et al. 2005; Bloom et al. 2006). This diversity in environments almost certainly reflects differing progenitors for the LGRBs and SGRBs (Bloom & Prochaska 2006). Indeed, in the majority of LGRBs at low redshift it has been possible to isolate the signature of a Type Ic supernova, suggesting that their progenitors are Wolf–Rayet stars (Hjorth & Bloom 2011, and references therein). In contrast, deep searches in SGRBs at similar redshift fail to locate any such signatures, and offer further evidence that the progenitors of short bursts are not related to stellar core collapse (Hjorth et al. 2005; Bloom et al. 2006; Rowlinson et al. 2010a). The varied host demographics offer part of the picture, but the locations of the bursts on their hosts are also greatly diagnostic. It appears that short bursts are scattered significantly on their hosts, occurring in typically fainter regions, and at larger offsets than their long cousins (Fruchter et al. 2006; Fong, Berger & Fox 2010; Church et al. 2011). These properties can naturally be explained if the progenitor is a merger of two compact objects [e.g. neutron star–neutron star (NS), collapsing to a black hole by accretion-induced collapse (AIC) or neutron star–black hole (BH)] (Eichler et al. 1989; Bloom, Sigurdsson & Pols 1999; Fryer, Woosley & Hartmann 1999;

★ E-mail: R.L.Tunnicliffe@warwick.ac.uk

[1] Usually taken as those with $T_{90} < 2$ s, where T_{90} is the time over which 90 per cent of the prompt gamma-ray emission is observed. As a class, the SGRBs also have harder spectra than LGRBs, but there is significant scatter.

Fong et al. 2010). This model has proved extremely hard to test observationally, although the recent discovery of a possible kilonova in the SGRB 130603B offers support for the model for at least some SGRBs (Berger, Fong & Chornock 2013; Tanvir et al. 2013).

A key distinguishing factor between different intrinsically ancient progenitor populations, such as AIC of white dwarfs to neutron stars (Levan et al. 2006a; Metzger, Thompson & Quataert 2007) and compact binary mergers, comes from the dynamics of the systems themselves. In a double compact object binary, a combination of natal kicks, and mass-loss from the binary at the time of each supernova, can act to provide the systems with space velocities of several hundred km s^{-1} (e.g. Wong, Willems & Kalogera 2010). Integrated over the lifetime of the binary of 10^7–10^{10} yr this can correspond to distances of tens of kpc from their birth sites, although the fraction of binaries that attain these distances remains uncertain (Belczynski et al. 2006; Church et al. 2011). For extremely high kicks, or relatively low-mass host galaxies, the binary may escape the galactic potential of its host altogether. Hence, a population of SGRBs in intergalactic space would offer strong support for a binary merger model for their progenitors (Bloom & Prochaska 2006; Berger 2010).

However, determining the offset of a burst from its host is non-trivial when there is no obvious parent galaxy coincident with or close to the burst location, i.e. where there is no outstanding candidate with an extremely low probability of chance alignment. Probabilistic methods based on the sky density of galaxies are often used to argue for a host association (e.g. Bloom et al. 2002, 2007; Levan et al. 2007; Berger 2010). However, the sky density is such that for any random position on the sky is likely to be within a few arcseconds of a galaxy with $R < 25$. In other words, in many cases we cannot *strongly* identify the host galaxy (probability of $\lesssim$1 per cent), which can lead to misidentifications. A second problem is that to the limits of our ground-based [or even *Hubble Space Telescope* (*HST*)] observations, we probe a reducing fraction of the galaxy luminosity function as we move to higher redshift. Hence there is a potential for confusion between GRBs which have been kicked far, and hence are well offset, from relatively local hosts and those which lie within fainter galaxies at high redshifts. This problem is particularly acute if the high redshift galaxies host primarily old stellar populations, and hence exhibit only weak rest-frame UV (observer-frame optical) emission.

In this sense, the 'hostless' problem for SGRBs is not that there are a lack of candidate hosts; in all lines of sight there will be plausible parent galaxies within a few tens of kpc in projection. Frequently, the probability of chance alignment with at least one of these is small, and may be suggestive of kicks to the SGRB progenitors (Berger 2010). Instead, the problem in these hostless cases is the difficulty in determining uniquely the parent galaxy (from e.g. several with similar probabilities, or underlying larger scale structure). This means we are unable to make full use of the diagnostic information contained in the offset distribution and the properties of the hosts for improving our knowledge of SGRB progenitors.

Obtaining the redshift for the GRB using the afterglow would allow us to narrow our search to hosts within a small redshift range. However, for short bursts the faintness of their afterglows (Kann et al. 2011) means that redshifts are difficult to obtain in practice, and in nearly all cases to-date redshifts for SGRBs have been inferred from their presumed host galaxy rather than from the burst itself (e.g. Berger et al. 2005; Hjorth et al. 2005; Rowlinson et al. 2010a; Fong et al. 2011a). In fact, even accounting for the faint continuum, in some cases the lack of any absorption features also gives an indication that the burst is not in a dense interstellar medium (Piranomonte et al. 2008; Berger et al. 2010).

Based on the optically localized SGRB sample outlined in Section 3.1 with details in Appendix A, ∼70 per cent have apparently well-associated host galaxies, while the remainder are apparently hostless. This may offer evidence for kicks. Here, we present the discovery and subsequent observations of the optical afterglows and host limits of a further two hostless bursts, GRB 090305A (see also Berger 2010 and Nicuesa Guelbenzu et al. 2012), GRB 091109B and deep limits to a third, GRB 111020A (see also Fong, Berger & Fox 2011b). These GRBs are all unambiguously of the short-hard class, with $T_{90} < 0.5$ s and prompt emission which is spectrally hard. Indeed, even given the recent work suggesting a shorter dividing line between the SGRB and LGRB populations (Bromberg et al. 2013), these bursts would remain in the short-hard class. We consider the extent to which our current detection limits probe the galaxy luminosity function as a function of redshift, and what this implies for hostless GRBs more generally.

These hostless GRBs could reside within relatively high-redshift (but so far unseen) host galaxies or have travelled far from their low-redshift ($z < 1$) hosts, perhaps within the intergalactic medium (IGM). Clues to their origins may come from studies of the most likely hosts amongst the nearby galaxies on the sky.

We present an alternative diagnostic tool developed by taking random positions and comparing them to the distribution of galaxies on the sky, thus reproducing the sort of analysis performed when looking for a short GRB host. From this, we directly determine the chance probability of association ($P_{\rm chance}$) and a radius within which we can confidently state a host association. Doing this avoids assumptions as to the functional form of the number counts, and naturally encapsulates field to field variance and clustering, resulting in more robust assessments of the chance probability than the traditional route of using number counts alone.

2 OBSERVATIONS AND ANALYSIS

2.1 GRB 090305A

2.1.1 Prompt and X-ray observations

GRB 090305A was detected by the Burst Alert Telescope (BAT) instrument on *Swift* (Barthelmy et al. 2005a) in 2009 March 05 at 05:19:51 UT (Beardmore et al. 2009a). The GRB had a duration of $T_{90} = 0.4 \pm 0.1$ s and a fluence (15–150 keV) of $7.5 \pm 1.3 \times 10^{-8}$ erg cm^{-2} with the errors quoted at the 90 per cent confidence level (Krimm et al. 2009). For a GRB at $z = 0.3$ (a typical redshift for an SGRB) extrapolating this fluence to the 1–1000 keV range gives an isotropic equivalent energy of $E_{\rm iso} = 1.6 \times 10^{50}$ erg.

The X-ray Telescope (XRT) on *Swift* (Burrows et al. 2005) began observations 103.4 s after the BAT trigger in photon counting (PC) mode but no X-ray afterglow was detected (Beardmore et al. 2009b). An optical afterglow was detected by the Gemini Multi-Object Spectrograph (GMOS) instrument on the Gemini-South telescope (Hook et al. 2004) at position $\alpha = 16^{\rm h}07^{\rm m}07\overset{\rm s}{.}58$, $\delta = -31^\circ33'22\overset{''}{.}1$ (Cenko et al. 2009). Using the position provided by the Gemini observations and by relaxing the default screening criteria, the X-ray afterglow was identified with 99.99 per cent confidence using the method of Kraft, Burrows & Nousek (1991) for determining confidence limits with a low number of counts. The source was no longer detected when further XRT measurements were made 3.92 ks after the BAT trigger for 2.05 ks. Using all available data this gives a 3σ upper limit of 1.7×10^{-3} count s^{-1}, indicating a decay slope of at least ∼0.8 (Beardmore et al. 2009b). All BAT and XRT measurements and limits are shown in Fig. 1.

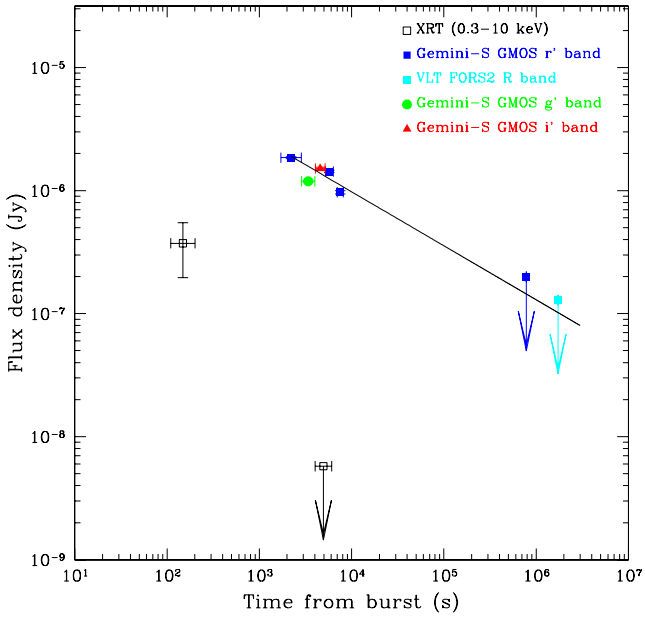

Figure 1. X-ray and optical light curve of GRB 090305A. The XRT measurements are shown as black open squares including the single XRT detection and late time upper limit (Evans et al. 2007). The Gemini-S GMOS optical measurements and limit in the r', g' and i' bands are the blue filled squares, green circle and red triangle, respectively. The VLT R-band limit is shown as a cyan square. Fitting a single power law to the r' band, where we have three detections and an upper limit, yields a decay index of $\alpha_r = 0.44 \pm 0.02$, shown on the plot. This is a poor fit to the data but with only three detections it is difficult to constrain the slope.

2.1.2 *Optical observations*

Multiple observations of the field of GRB 090305A were obtained using the Gemini South telescope as well as independently detected with the GROND instrument on 2.2 m telescope at La Silla Observatory (see Nicuesa Guelbenzu et al. 2012 where they also investigate the Gemini afterglow). The optical afterglow was detected in all bands, as reported by Cenko et al. (2009), with observations being made ∼35, ∼55 and ∼75 min after the GRB in the r', g', i' bands, respectively. Furthermore, observations were made in the r' band ∼95, ∼125 and ∼13 000 min (∼9.02 d) after the BAT trigger with the afterglow still detected in the first two epochs. The final Gemini epoch can be used to place a constraint on any host galaxy coincident with the GRB position, with the limit measured using an aperture equivalent to the full width at half-maximum of the image. The r' band images are shown in Fig. 2 with the optical transient (OT) and nearby source A indicated. Variation of the afterglow flux density, F, is described using $F \propto t^{-\alpha}\nu^{-\beta}$. The spectral fit using the r'-, g'- and i'-band detections has an index of $\beta_O \sim 0.57$. The temporal fit to the r'-band detections has slope of $\alpha_r = 0.44 \pm 0.02$, shown in Fig. 1, although this is a poor fit the limited number of points preclude the fitting of more complex models.

A final epoch of observations was made using the FOcal Reducer and low-dispersion Spectrograph (FORS2) instrument on the Very Large Telescope (VLT) in the R band. This was a long exposure image but due to the proximity of a group of bright stars could only marginally improve on the Gemini limit. Details of all observations made are listed in Table 1.

2.2 GRB 091109B

2.2.1 *Prompt and X-ray observations*

GRB 091109B was detected by the BAT instrument on 2009 November 09 at 21:49:03 UT (Oates et al. 2009a). The *Suzaku* Wide-band All-sky Monitor, which also detected this GRB, measured an $E_{\rm peak} = 1330^{+1120}_{-610}$ keV showing the GRB is spectrally hard (Ohno et al. 2009). The GRB had a duration of $T_{90} = 0.3 \pm 0.03$ s and a fluence (15–150 keV) of $1.9 \pm 0.2 \times 10^{-7}$ erg cm^{-2} (Ohno et al. 2009). As for GRB 090305A, if we use a redshift of $z = 0.3$ and extrapolate this fluence to the 1–1000 keV range we measure an isotropic equivalent energy of $E_{\rm iso} = 5.11 \times 10^{50}$ erg.

The X-ray afterglow was detected by the XRT which began observing at 21:50:21.1 UT, 78.1 s after the BAT trigger (Oates et al. 2009a). The X-ray light curve shown in Fig. 3, with data entirely taken in PC mode, can be fit by a power law with decay index $\alpha_X = 0.637^{+0.086}_{-0.084}$ (90 per cent errors).

2.2.2 *Optical observations*

We obtained multiple observations of the GRB position in the R band using the FORS2 instrument and observations in the J and K band using the High Acuity Wide field K-band Imager (HAWK-I) instrument both on the VLT.

We discovered an optical afterglow in the R band from two sets of R-band observations taken on 2009 November 11, ∼360 and ∼620 min after the BAT trigger with clear fading between the epochs (Levan et al. 2009; Malesani et al. 2009). The position was $\alpha = 07^{\rm h}30^{\rm m}56\overset{\rm s}{.}60 \pm 0.02$, $\delta = -54^\circ05'23\overset{''}{.}3 \pm 0.3$, consistent with the revised X-ray position (Evans et al. 2009). A third set of R-band observations were taken on 2009 November 11, ∼1900 min (∼1.32 d) after the start of the GRB and when the afterglow had faded allowing us to place a constraint on the magnitude of any underlying host galaxy. These images are shown in Fig. 4 with the

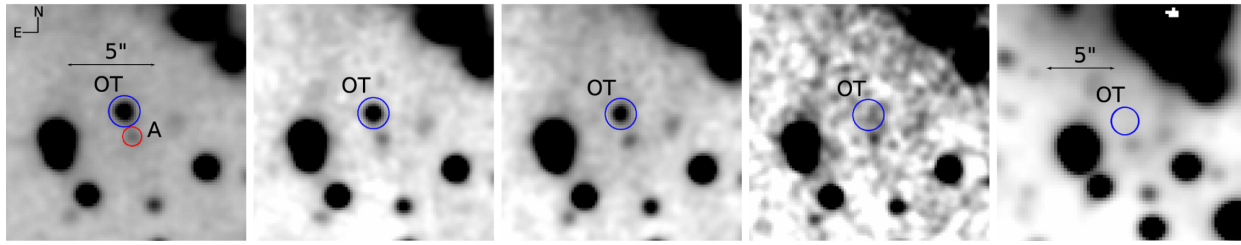

Figure 2. A finding chart for GRB 090305A. All images except the final image are from Gemini r'-band observations and show the optical transient (OT; blue circle) fading. No coincident host galaxy is found from late time Gemini imaging at the GRB position. The potential host galaxy, source A, is identified in the first epoch image with a red circle. Due to the faintness of source A, it is not possible to determine whether it is extended. The final image is from our additional late time observation using the FORS2 instrument on the VLT and also shows the lack of a coincident host galaxy down to the limits of the image.

Table 1. A log of Gemini and VLT observations of GRB 090305A. Magnitudes quoted for the Gemini telescope are in the AB system and for the VLT are in the Vega system. These magnitudes have been calibrated from the standard Gemini zero-points. Photometric errors are statistical only. All magnitudes have been corrected for Galactic extinction of $E(B-V) = 0.22$ (Schlegel, Finkbeiner & Davis 1998).

Start of observations	Exposure time	Mid-point ΔT (min)	Instrument	Filter	Magnitude
2009-03-05 05:47:23.5	5 × 180 s	36.87	Gemini-South GMOS	r'	23.26 ± 0.02
2009-03-05 06:07:00.6	5 × 180 s	56.51	Gemini-South GMOS	g'	23.74 ± 0.03
2009-03-05 06:26:41.5	5 × 180 s	76.19	Gemini-South GMOS	i'	23.48 ± 0.03
2009-03-05 06:46:21.2	5 × 180 s	95.84	Gemini-South GMOS	r'	23.54 ± 0.02
2009-03-05 07:07:20.5	4 × 500 s	125.53	Gemini-South GMOS	r'	23.96 ± 0.03
2009-03-16 05:37:04.7	10 × 150 s	∼13 000	Gemini-South GMOS	r'	>25.69
2009-03-25 05:08:06.8	20 × 240 s	∼28 830	VLT FORS2	R	>25.90

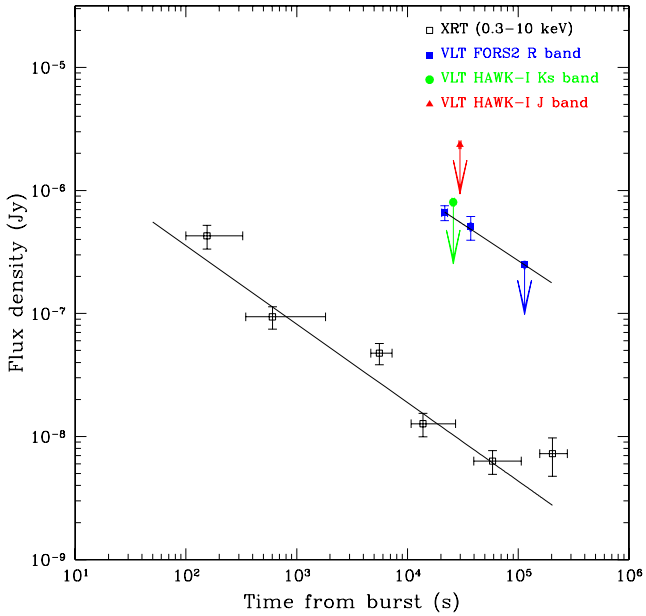

Figure 3. The XRT (Evans et al. 2007) and VLT optical light curves for GRB 091109B. The X-ray data is plotted as black open squares and the *R*-band optical measurements and limits are plotted as blue filled squares. Additional *J*- and *K*-band limits from the HAWK-I instrument on the VLT are plotted as a red triangle and a green circle, respectively. Both the X-ray and the *R*-band data have been fitted with power slopes giving decay indices of $\alpha_X = 0.637^{+0.086}_{-0.084}$ and $\alpha_R = 0.60 \pm 0.10$, consistent with each other.

OT indicated in the image along with two potential host galaxies: nearby faint source A and bright galaxy, source B.

J- and *K*-band observations were also made on 2009 November 10, ∼495 and ∼430 min after the GRB, respectively. The transient was not detected in either band. The upper limit placed in the *K*-band implies that the afterglow emission was unusually blue, with a practically flat spectral energy distribution (SED), and therefore suggestive of low extinction. We note that this is also unusual in the context of the afterglow model where we would expect a steeper slope of at least $\beta = 1/2$ (Sari, Piran & Narayan 1998). All observations, magnitudes and limits are listed in Table 2 and shown in Fig. 3. The X-ray and optical temporal decay indices are $\alpha_X = 0.59 \pm 0.05$ and $\alpha_R = 0.60 \pm 0.10$, where the X-ray slope is consistent with that reported by Evans et al. (2009).

2.3 GRB 110112A

2.3.1 *Prompt and X-ray observations*

Swift detected GRB 110112A with the BAT instrument on 2011 January 12 at 04:12:18 UT (Stamatikos et al. 2011). The duration of the GRB was $T_{90} = 0.5 \pm 0.1$ s and it had a fluence (15–150 keV) of $3.0 \pm 0.9 \times 10^{-8}$ erg cm^{-2} (Barthelmy, Sakamoto & Stamatikos 2011).

An X-ray afterglow was detected by the XRT which started observing 75.5 s after the BAT trigger (Stamatikos et al. 2011).

2.3.2 *Optical observations*

An OT was detected ∼15.4 h after the BAT trigger in the i' band using the Auxiliary-port camera (ACAM) on the William Herschel Telescope (WHT). This object was marginally coincident with the position for a candidate identified by Xin et al. (2011) with the Tsinghau National Astronomical Observatories of China Telescope (TNT) at Xinglong Observatory, whose brighter magnitudes implies fading (Levan, Tanvir & Baker 2011). This object was not detected in late-time imaging using the GMOS instrument at the Gemini-South telescope confirming this object as the afterglow of the GRB.

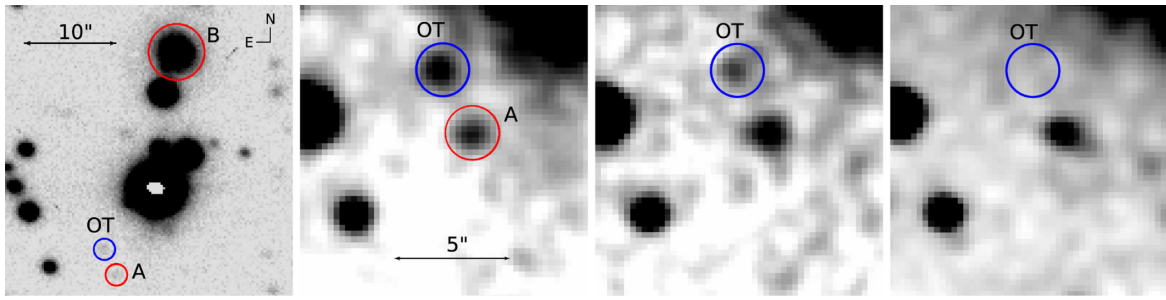

Figure 4. Finding chart for GRB 091109B. The images were taken in the *R_SPECIAL* filter on the VLT. The first two panels are from the first epoch and indicate the optical transient (OT), a nearby source (A) and a bright galaxy (B). The optical transient can clearly be seen to be fading across the three epochs. Other objects visible in the field appear to be foreground stars and not galaxies.

Table 2. A log of VLT FORS2 and HAWK-I observations of GRB 091109B. Magnitudes are in the Vega system and have been corrected for Galactic absorption of $E(B-V) = 0.17$ (Schlegel et al. 1998). Photometric errors are statistical only.

Start of observations	Exposure time	Mid-point ΔT (min)	Band	Magnitude
2009-11-10 03:28:37.800	8×300 s	361.56	*R*	24.13 ± 0.14
2009-11-10 04:53:49.091	$22 \times 10 \times 6$ s	431.95	*K*	>22.23
2009-11-10 05:54:57.305	$22 \times 10 \times 6$ s	497.45	*J*	>21.99
2009-11-10 07:59:36.965	4×300 s	621.39	*R*	24.42 ± 0.21
2009-11-11 05:10:38.044	8×300 s	1903.28	*R*	>25.63

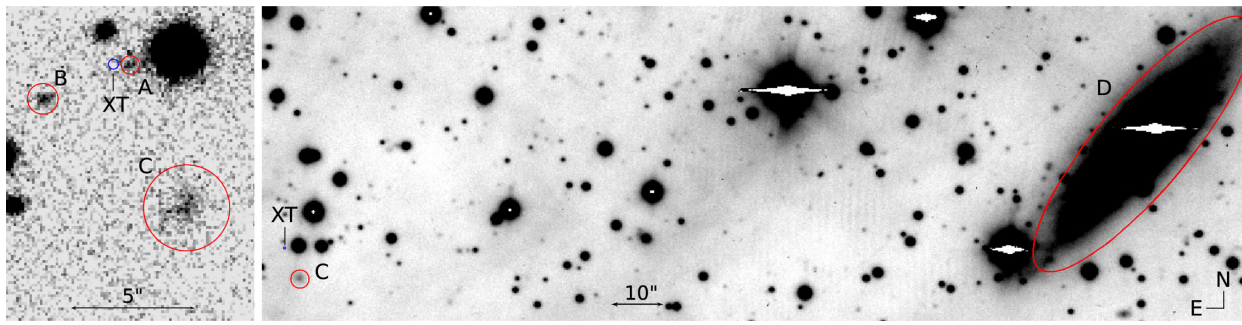

Figure 5. VLT observations for GRB 111020A. The early time *J*-band image is shown on the left with three nearby objects (A, B, C) shown in relation to the position of the X-ray transient (XT) with no infra-red transient detected. Objects A, B, C are synonymous with objects G3, G2, G1, respectively, identified in Fong et al. (2012). Though objects B (G2) and C (G3) show evidence for extension, the faintness of object A (G1), the object closest to the X-ray position, makes this difficult to determine and the afterglow is still clearly offset from this object. In the FORS $R_{SPECIAL}$ band image shown on the right of the three objects we only detect galaxy C. In addition, we detect, a nearby large spiral galaxy (labelled D).

For further details of observations of GRB 110112A, see Fong et al. (2013).

2.4 GRB 111020A

2.4.1 Prompt and X-ray observations

GRB 111020A was detected by the BAT instrument on 2011 October 20 at 06:33:49 UT (Sakamoto et al. 2011b). The duration of the GRB was $T_{90} = 0.40 \pm 0.09$ and it had a fluence (15–150 keV) of $6.5 \pm 1.0 \times 10^{-8}$ erg cm^{-2} (Sakamoto et al. 2011a). Extrapolating this fluence to the 1–1000 keV range, using a redshift of $z = 0.3$, we measure an isotropic equivalent energy of $E_{\rm iso} = 6.15 \times 10^{49}$ erg.

The X-ray afterglow was detected by the XRT which started observing 72.8 s after the BAT trigger (Sakamoto et al. 2011b). The afterglow was also observed by the *Chandra* X-ray Observatory which placed the most precise position on the afterglow: $\alpha = 19^{\rm h}08^{\rm m}12\overset{\rm s}{.}49 \pm 0.2, \delta = -38^\circ00'42\overset{''}{.}9 \pm 0.2$ (Fong et al. 2012).

2.4.2 Optical and Infrared observations

Observing with the Gemini-South telescope in the i' band Fong et al. (2011b) noted the presence of several point sources near to the X-ray afterglow position. However, with further imaging Fong & Berger (2011) later reported that none of these sources were fading between the epochs. Hence, no optical afterglow was observed for this GRB.

We obtained observations of GRB 111020A with the VLT, equipped with HAWK-I in the *J* band. Our observations started at 00:33 on 2011 October 21, approximately 18 h after the burst with a total exposure time of 44 min on sky. We identify the same sources seen by Fong et al. (2012) (in particular G1, G2 and G3). In our imagery, we label these objects A (G3), B (G2) and C (G1) in order of increasing offset from the GRB position. We note that only object C and perhaps B appears extended in our image with 0.4 arcsec seeing. We do not identify any additional sources which are likely IR afterglow of GRB 111020A to a limiting magnitude of $J = 23.6$ (3σ).

We obtained late time observations of the GRB position in the *R* band using the FORS2 instrument on the VLT. This observation is shown in Fig. 5 and the details of the observation are given in Table 3. Although no optical counterpart was found, due to the small error (sub-arcsecond) on the *Chandra* X-ray afterglow position, we can still use this to accurately measure offsets from any potential host galaxies and to place deep limits at the position of the afterglow.

Additionally at this epoch, we obtained FORS2 spectroscopy of a bright galaxy offset from the GRB position which is a plausible host (see Section 2.5) shown in Fig. 6. The spectrum is significantly contaminated by light from a bright foreground star overlapping the galaxy and confused with its nucleus. However, in the outlying regions of the galaxy we identify a weak emission line at 6688 Å. Identifying this as H$-\alpha$ suggests at redshift of $z = 0.019$, or 81 Mpc.

2.5 Candidate host galaxies

For GRB 090305A, GRB 091109B, GRB 110112A and GRB 111020A there is no host galaxy coincident with the optical afterglow position down to deep limits. Hence, we investigate galaxies in the field around these SGRBs to determine if there are any strong host galaxy candidates. GRB 090305A occurred in a region with a high density of sources, meaning there are many field objects of the order of 5–8 arcsec away, none of which show evidence of extension. There is a faint object located 1.48 arcsec from the optical afterglow, shown in Fig. 2 and labelled as source A. The magnitude of source A is $r' = 25.64 \pm 0.20$. Due to its faint magnitude it is not possible to determine with high confidence whether this object is extended.

Table 3. A log of VLT HAWK-I and FORS2 observations of GRB 111020A in the *J* and *R_SPECIAL* filters. The HAWK-I observation was made at early times with no afterglow detected. Both observations allow us to place a constraint on any underlying host galaxy. The magnitudes quoted here are in the Vega system and have been corrected for Galactic absorption of $E(B-V) = 0.43$ (Schlegel et al. 1998). Photometric errors are statistical only.

Start of observations	Exposure time	Mid-point ΔT (d)	Band	Magnitude
2011-10-21 00:33:29.579	$44 \times 10 \times 6$ s	0.772 13	*J*	>23.6
2012-03-23 07:18:05.768	20×240 s	155.03	*R*	>24.03

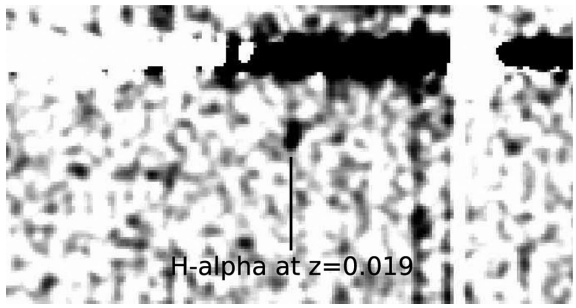

Figure 6. The VLT/FORS spectrum of the galaxy proximate to GRB 111020A. The source is significantly contaminated by an extremely bright foreground star sitting close to the location of the nucleus of the galaxy. We have attempted to remove this star by subtracting the median value across the wavelength range in each row from the spectrum. At an offset position, consistent with the disc of the galaxy we do observe an emission line at 6690 Å. If this line is interpreted as Hα, the inferred redshift is $z = 0.019$.

For GRB 091109B, we identified two extended objects which are potential host galaxies. The first is a faint object ∼3.0 arcsec from the GRB position marked in Fig. 4 as source A with $R = 23.82 \pm 0.10$. The object is not detected in the *J* and *K* band down to the limiting magnitude listed in Table 2. The second potential host, source B, is a spiral galaxy located ∼22.5 arcsec from the GRB position. Even though this is located much further from the GRB position than source A, it is much brighter with magnitudes $R = 19.19 \pm 0.05$, $J = 17.45 \pm 0.05$ and $K = 16.16 \pm 0.05$.

GRB 110112A occurred in a relatively clear region quite well offset from other objects in the field. We find three spiral galaxies which could potentially be host galaxies labelled as A, B and C in Fig. 7. These objects have i'-band magnitudes of 22.70 ± 0.07, 21.16 ± 0.04 and 20.17 ± 0.05, respectively, with increasing offsets of 12.9, 19.3 and 35.6 arcsec.

In our images, we identify four objects which could be candidate host galaxies for GRB 111020A, shown in Fig. 5. Three of these objects are within 7 arcsec of the X-ray afterglow with the fourth being a large, extremely bright spiral galaxy at an offset of 166 arcsec. The labels of A–D are with increasing offset from the afterglow position. This galaxy, labelled D in our image, has a magnitude $R \sim 14.0$ with the uncertainty due to a number of saturated foreground stars obscuring the galaxy, making it difficult to make a precise measurement. Our measured redshift for the galaxy (if taken from the single line) is $z = 0.018$, corresponding to a projected separation of 60 kpc. The three objects nearby have offsets of 0.7, 3.0 and 6.8 arcsec, respectively, labelled as A, B, C in Fig. 5 corresponding to galaxies G3, G2 and G1 in Fong et al. (2012). All these objects are detected in our HAWK-I data with magnitudes $J = 22.00 \pm 0.09$, 21.41 ± 0.10 and 20.70 ± 0.08, respectively, but with only objects B, C showing evidence for extension. However, only object C is clearly detected in our FORS data with $R = 21.34$ and object B marginally detected.

To give an indication of whether these galaxies are strong candidates to be the host, we ask what is the probability, $P_{\rm chance}$, that an unrelated galaxy of the same magnitude or brighter would be found within the given offset. This approach has been considered extensively for LGRBs and SGRBs (e.g. Bloom et al. 2002; Levan et al. 2008; Berger 2010). Here, we use a simplified version based on the offset between the SGRB position and the given galaxy and compare this to the distribution of such offsets in a large sample of random sky positions, as described in Section 3.3. For source A associated with GRB 090305A, we measure a value of $P_{\rm chance} = 0.09$ which, though a low value, does not provide a firm host association. Similarly, for GRB 091109B sources A and B have values of $P_{\rm chance} = 0.09$ and 0.10, respectively. For GRB 110112A, all three host candidates have relatively higher $P_{\rm chance}$ values of 0.50, 0.34 and 0.42 with galaxy B having the lowest $P_{\rm chance}$ value.

Looking at the objects, we detect in the field of GRB 111020A, in both our *R*- and *J*-band data, we find $P_{\rm chance}$ values of 0.007, 0.04, 0.09 and 0.05 for objects A (G3), B (G2), C (G1) and D. If object A (G3) is indeed a galaxy then this object is strongly associated and hence the GRB could be classified as 'hosted'. However, we caution that this field is at low galactic latitude and that this object could be faint star. In addition, this object does not show significant

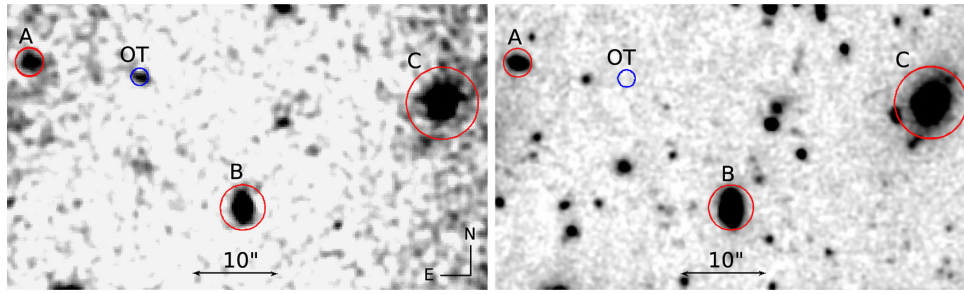

Figure 7. Finding chart for 110112A. The images from the WHT ACAM instrument (left) and the Gemini-South GMOS instrument show the position of the optical transient (OT) and three potential host galaxies (A, B, C). These objects show evidence for extension.

evidence for extension and so we do not conclusively rule out the other galaxies as potential hosts.

3 IDENTIFYING HOSTLESS SGRBs

3.1 A sample of SGRBs

We utilize a sample of all SGRBs detected up to 2012 April. This includes bursts with $T_{90} < 2$ s, and those bursts which have been declared short bursts with extended emission by the *Swift* team in the GCN circulars archive. Since we are interested in host identifications, we further cull this input list to require at least an XRT detection of the afterglow, since BAT-only positions are insufficient to identify hosts with moderate to high confidence unless they are extremely bright (e.g. Levan et al. 2008). In addition, since we are interested in the host galaxies of these SGRBs, we do not list XRT-localized SGRBs where a host galaxy search has not been reasonably attempted.

By these criteria the sample includes 40 GRBs: 33 SGRBs with $T_{90} < 2$ s and 7 with extended emission. Of these GRBs 26 are well-localized and 14 are localized using the XRT. Our complete host galaxy sample along with some basic properties of the GRBs is shown in Tables A1 and A2.

3.2 Difficulties of host identification

Probabilistic arguments of the sort outlined above have been used to argue for a host galaxy associations for many *Swift* SGRBs (e.g. Prochaska et al. 2006; Kocevski et al. 2010; McBreen et al. 2010; Rowlinson et al. 2010a). However, $P_{\rm chance}$ is calculated as an independent quantity for each galaxy considered, meaning that for some SGRBs there are several galaxies with roughly similar $P_{\rm chance}$ values. For example, there may frequently be multiple galaxies in the field for which $P_{\rm chance} < 5$ per cent (e.g. Levan et al. 2007), but in these cases this clearly does not represent the true false positive rate for a given burst (since at most one can be the true host). This potentially produces a degeneracy in identification of candidate hosts between bright galaxies with large offsets and faint (or even undetected) galaxies with small offsets (Berger 2010), as seen for GRBs 091109B and 111020A.

Such problems may be largely unavoidable for any population of events that arises at large offsets; however, our prior expectations may impact the likelihood assigned to either the kicked or high-redshift (and undetected host) scenarios. For example, the association of LGRBs with massive star collapses mean that the non-detections of hosts to deep limits in LGRBs are typically ascribed to faint host galaxies, with the expectation that deep observations will ultimately find them underneath the burst positions (e.g. Hjorth et al. 2012; Tanvir et al. 2012). For short GRBs the models are far less well constrained. It is clear that within the population that lie on host galaxies, the positions are not associated strongly with active star formation (Fong et al. 2010), and therefore the progenitors can likely have longer lifetimes than those of LGRBs. The population of SGRBs identified to date also has a much lower mean redshift than for LGRBs ($\langle z \rangle \sim 0.7$ compared to $\langle z \rangle \sim 2.2$) (Jakobsson et al. 2006, 2012; Fong et al. 2010), if this distribution is representative of the underlying distribution then it is more likely that observations of a given depth would uncover the host galaxy (see Section 4.1). Given this, it is natural to also consider the difficulties that may arise identifying hosts from a kicked population.

To demonstrate the difficulties in the kicked scenarios, we can consider the likely implications of a binary merger model for the locations around a given galaxy. Indeed, if NS binary mergers are indeed responsible for the creation of SGRBs then we may expect larger offsets due to both the natal kick and the delay in merger time after creation (potentially $>10^{10}$ yr), although some authors have argued for much shorter delays for the bulk of the population (Belczynski et al. 2006). Fig. 8 shows typical NS binary merger sites with respect to a spiral host galaxy with $R = 23$ at $z = 1$, comparable in luminosity ($M_B \sim -20.4$) to the Milky Way (from Church et al. 2011). We include both the case of NS binary systems formed through a primordial channel and a dynamical channel within globular clusters (GCs), where a neutron star captures a companion through three-body interactions (Grindlay, Portegies Zwart & McMillan 2006), i.e. we also plot the distribution of GCs. We compare this with the $P_{\rm chance}$ values we would measure as a function of projected offset (in kpc) for this particular case of a galaxy with $R = 23$ at $z = 1$. We also highlight the areas where $P_{\rm chance}$ is 2 per cent and 5 per cent. This demonstrates that for this model of NS binary mergers, we may expect a significant fraction to merge at a point where we can no longer associate the resulting explosion with the host galaxy from which it originated (see also Berger 2010). This problem becomes even more acute when considering fainter galaxies. A lower luminosity galaxy at the same redshift will have significantly higher $P_{\rm chance}$ at moderate offsets, making a firm association difficult.

In other words, in any kicked scenario we would expect a significant fraction of bursts for which we cannot identify any host galaxy. The implications this could have for hostless GRBs are further discussed in Section 4.2.

3.3 A diagnostic tool to help investigate short burst host associations

Given the above limitations, we take an alternative approach to calculating $P_{\rm chance}$, by directly calculating for multiple random positions on the sky. We took 15 000 random positions within the footprints of the Sloan Digital Sky Survey (SDSS; Abazajian et al. 2009) and the Cosmological Evolution Survey (COSMOS; Capak et al. 2007), and used the measured galaxy data available within these surveys to find the nearest galaxies brighter than a given magnitude. The galaxy magnitude range chosen was reflective of SGRB host galaxies, using SDSS data at the bright end (15–22 mag) and supplementing this with data from the Subaru telescope in the COSMOS survey at the faint end (>22 mag). We excluded any SDSS positions with Galactic extinction values $E(B-V) > 0.1$ and corrected for Galactic extinction for all galaxy magnitudes within the sample. For the COSMOS sample, we utilize galaxy magnitudes measured within a 3 arcsec fixed aperture since for faint galaxies this should enclose essentially all of the light.

The galaxy distribution is shown in Fig. 9 along with the enclosing percentiles (1, 5, 10, 15 and 50 per cent percentiles) of the distribution, i.e. beyond the 1 per cent line only 1 per cent of the galaxies in the sample have magnitude $<r'$ and are at offset $<$ observed. Also shown are the putative host galaxies of the SGRB population. We would expect any well constrained host galaxy (by $P_{\rm chance}$ or similar probabilistic measure) to be an outlier to the main galaxy distribution and, indeed, we see that all strongly associated SGRB host galaxies lie below the 1 per cent percentile line. For hostless GRBs, however, the proposed host galaxies lie closer to the background galaxy distribution.

We can use the division between GRBs strongly associated with their host galaxies and those considered hostless shown on Fig. 9 to define an 'association radius', δx. For a galaxy of a given

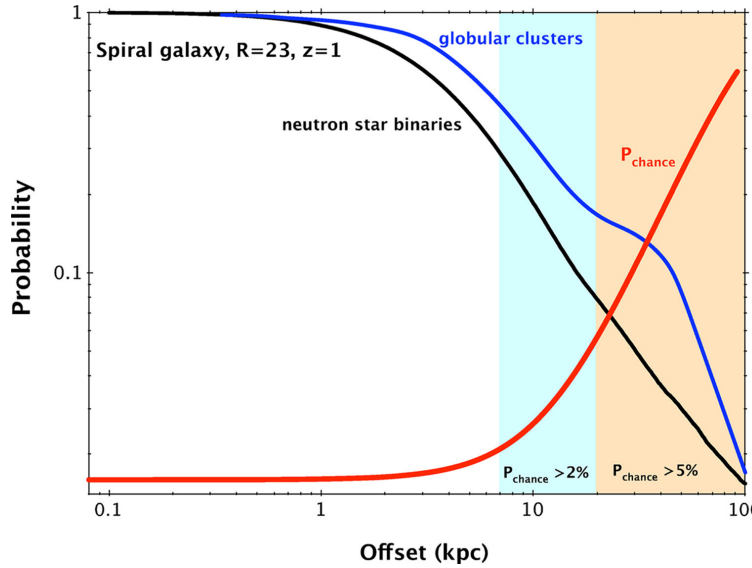

Figure 8. This plot shows the distribution of NS binary mergers with respect to a Milky Way-like spiral galaxy at $z = 1$. This is shown for both the primoridal and the dynamical channel of NS binary formation. The value of $P_{\rm chance}$ we would expect for this galaxy at $R = 23$ are also shown with the 2 per cent and 5 per cent $P_{\rm chance}$ areas highlighted.

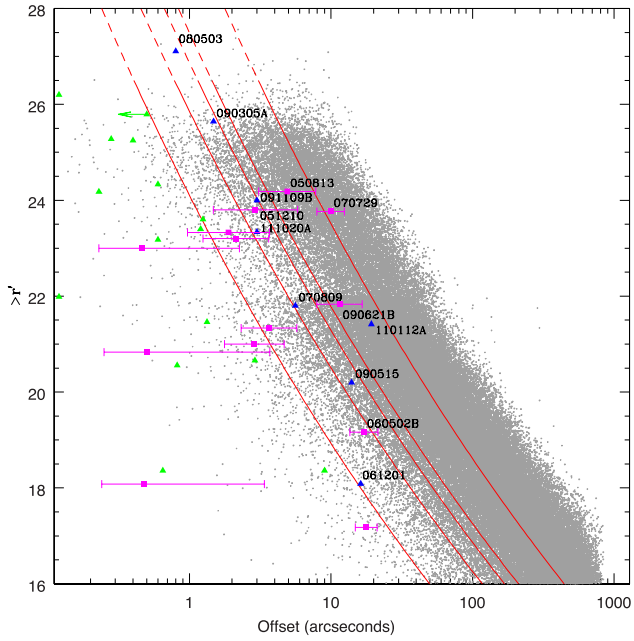

Figure 9. Using random positions in the Sloan Digital Sky Survey (SDSS) and the Subaru telescope in the Cosmological Evolution Survey (COSMOS), we have plotted the minimum offsets for galaxies brighter than a given r' magnitude for 15 000 random positions. The solid red lines are the 1, 5, 10, 15 and 50 per cent percentiles for this data set, with the dotted lines showing the extrapolation of the fit beyond our data set. We have plotted the galaxies with the lowest $P_{\rm chance}$ for all SGRBs with optical (or CXO) localizations (triangles) and for SGRBs with only *Swift*/XRT positions (purple squares). The blue triangles represent galaxies in the field of hostless SGRBs, with only one galaxy being included for each GRB. All well-constrained host galaxies (green triangles) lie below the 1 per cent percentile line.

magnitude, this is the offset from the centre of the putative host galaxy within which we can say the GRB is strongly associated, specifically there is a less than 1 per cent chance that an unrelated galaxy of this magnitude (or brighter) would appear within this distance. Conversely, if a GRB does not fall within this radius for *any* nearby galaxy then we chose to describe it as hostless. δx (in arcseconds) is given by equation (1).

$$\delta x = 1.48 \times 10^{13}\, m_r^{-\gamma}, \qquad (1)$$

where m_r is the r'-band magnitude of the suggested host galaxy and $\gamma = 9.53$ describes the best-fitting power-law dependence and is an empirical fit to the data. Hence, we can define a hostless short GRB where the position of the GRB (allowing for the error box) does not fall within the association radius of any nearby galaxies. The choice of association radius clearly depends on the minimum probability that one is prepared to accept (e.g. one could prescribe differing radii at different confidence levels). However, the 1 per cent contour is broadly applicable, and would suggest for our sample of ∼20 SGRBs, we may expect one to be falsely associated with a galaxy which is not its host. Using this approach, we identify a total of seven (eight) hostless SGRBs, 061201, 070809, 080503, 090305A, 090515, 091109B and 110112A (and potentially 111020A). We also note that GRB 111117A is very close to the 1 per cent boundary (Margutti et al. 2012).

We also note that four of the XRT-localized GRBs are hostless (i.e. the error bars due to the few arcsecond XRT positions do not cross the 1 per cent line): 050813, 051210, 060502B, 070729 and 090621B. For GRB 090621B, however, this may be due to the lack of a deep search, thus far.

We can now compare the galaxies with the lowest $P_{\rm chance}$ values ($P_{\rm chance,\,min}$) for our seven (eight with our potential host of GRB 111020A) bursts to the distribution of random locations on the sky. This will allow us to ascertain if this sample of events, originate from the underlying galaxy distribution, as might be expected for local, but kicked SGRBs, or are essentially uncorrelated, as might be expected for SGRBs originating from higher redshift. To do this for each random location, we identify the galaxy with the minimum $P_{\rm chance}$, and hence arrive at a distribution of $P_{\rm chance,\,min}$ for all random locations.

Measuring the $P_{\rm chance}$ value is done by calculating the lines for multiple percentiles using the same formulaic form as equation (1) but varying the coefficient values. The percentile lines themselves

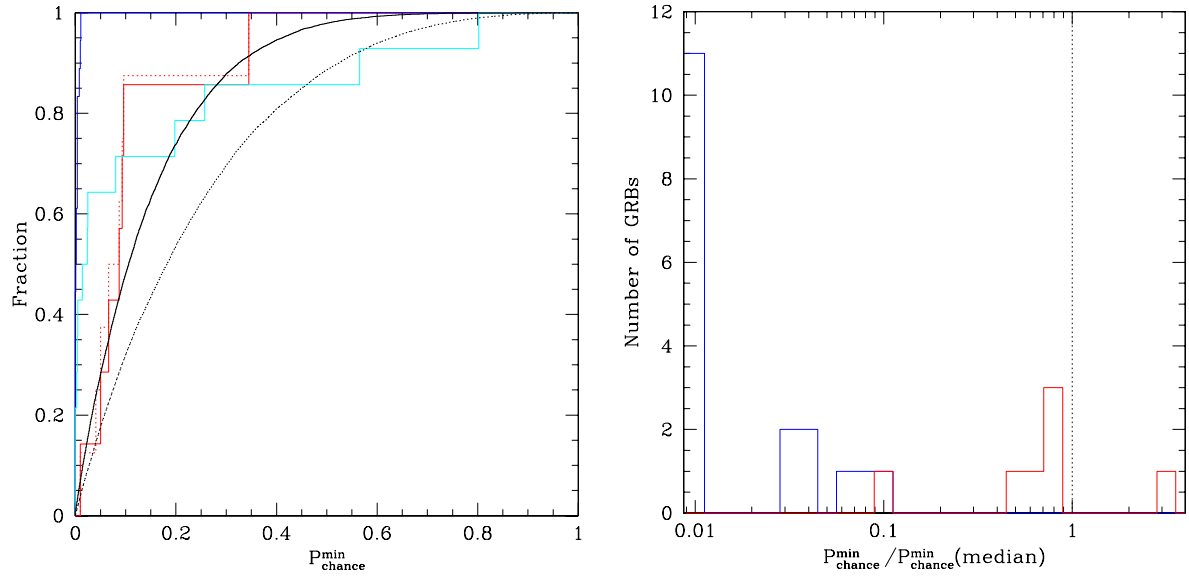

Figure 10. The plot on the left shows the cumulative distribution of $P_{\rm chance,\,min}$ for a set of 15 000 random positions within the SDSS and COSMOS footprints (black line). For comparison, the $P_{\rm chance,\,min}$ values calculated using the method of Bloom et al. (2002; dotted black line) are included. This is clearly distinct $P_{\rm chance}$ values calculated with the method outlined in the text. Also shown is the cumulative distribution of $P_{\rm chance,\,min}$ for the well-localized SGRBs with a host galaxy (blue), hostless SGRBs (red) and the *Swift*/XRT only detected SGRBs (cyan). The dotted red line is the hostless sample with the inclusion of an our identified galaxy (galaxy B) for GRB 111020A, but this is uncertain due to the presence of another object close-by which could be a faint star as explained in the text. The plot on the right shows a histogram of the ratios of the $P_{\rm chance,\,min}$ values to the median of the random galaxy distribution, for all the well-localized SGRBs in our sample. As for the plot on the right the hostless GRBs are shown in red and the other well-localized GRBs in blue. A KS test of these distributions compared to the random positions does not show that these populations are statistically distinct. However, looking at the median values does show that a significant fraction (6/7) of secure hostless cases the $P_{\rm chance,min}$ values are less than the median value for the random galaxy distribution.

can then be used to calculate the $P_{\rm chance}$ values. This is shown graphically in Fig. 10.[2] The KS probability that the hostless SGRB positions are drawn from an underlying random distribution of the sky is $P_{\rm KS} = 0.19$, which is not a rejection of this statement. We also show in Fig. 10 the curve that would be obtained from a calculation of $P_{\rm chance,\,min}$ via traditional routes utilizing only the number counts. The resulting curves are clearly different, this is particularly true at the low $P_{\rm chance,\,min}$ range, where the two curves differ by almost a factor of 2. Formally, the probability of this latter curve matching the observations is only $P_{\rm KS} = 0.01$, which is a rejection of the statement at $\sim 3\sigma$. In other words, the use of number counts alone can lead to an underestimate of the real probability of chance alignment of a galaxy with a given position on the sky.

As an alternative, we compare the $P_{\rm chance,\,min}$ values for the hostless GRBs to the median of the random galaxy distribution, looking only at galaxies above the limiting magnitude placed on each individual hostless GRB, we find that in 6/7 secure hostless cases (i.e. excluding GRB 111020A) the $P_{\rm chance,\,min}$ value is less than the median. Only in the case of GRB 110112A do we find that the $P_{\rm chance,\,min}$ value is greater than the median. For a random sky distribution, we would expect to sample this distribution evenly and the binomial probability of 6/7 (7/8) events lying at less than the median is 0.0547 (0.0313), again perhaps indicating that we are observing SGRBs from local structure in their fields.

Hence, these results are suggestive that we are observing SGRBs that are correlated with large-scale structure on the sky, even if the individual host galaxy that we identify with $P_{\rm chance,min}$ is not the true host. This may reflect that these bursts are kicked from relatively low redshift, and relatively luminous galaxies. However, it is also possible that we are observing these SGRBs from moderately massive structures at higher redshift, and hence the low values for $P_{\rm chance,min}$ are actually reflecting other cluster members. Early estimates from Berger et al. (2007a) put the percentage of SGRBs in clusters at $\sim$20 per cent (e.g. Bloom et al. 2006; Levan et al. 2008), though further studies of this nature have yet to be published.

Furthermore, the galaxies identified with lowest $P_{\rm chance}$ in these cases, are likely to be luminous (due to Malmquist bias), and may be massive (for an assumed mass to light ratio for a spiral galaxy), such galaxies are more likely to retain any dynamically kicked systems within their haloes. In contrast, lower mass galaxies have a much larger escape fraction, and are more likely to create a population of hostless SGRBs (see also Fryer et al. 1999; Bloom et al. 2002). Alternatively, the relative offsets from the galaxies with lowest $P_{\rm chance}$ means at least some GRBs may be residing within GC systems within these hosts. In this case, it may be that we are observing a population of dynamically formed binaries within these GCs, and that, given the typically large distances, we cannot directly observe the host cluster (e.g. Grindlay et al. 2006; Salvaterra et al. 2008; Church et al. 2011). Grindlay et al. (2006) predicts 10–30 per cent of SGRBs could be explained in dynamical mergers; however, as shown in Fig. 8 the majority of GCs are not at such large radii. Hence, while some of the hostless systems could arise from this channel, it seems unlikely that all of them would.

4 DISCUSSION

By considering the locations of SGRBs relative to random locations on the sky we have shown that even those SGRBs for which it is

[2] Note that although $P_{\rm chance,\,min}$ is strictly a function of the galaxy magnitude range considered, the span of galaxies covered by our joint SDSS/COSMOS analysis is fairly representative of the typical range accessible in our GRB host fields.

most difficult to unambiguously identify a host are likely to be at moderate redshift. However, it is possible that rather than observing the hosts themselves, we instead are tracing larger scale structure.

4.1 Constraints on the possibility of high-redshift host galaxies

We can use the 3σ point source detection limits at the locations of the hostless GRBs in our sample to place constraints on the possibility of a coincident host galaxy. For increasing redshift, we can determine the minimum galaxy luminosity, $L_{\rm lim}$ as a fraction of $L^{\star}$ (the characteristic luminosity of the knee of the Schecter luminosity function; Schechter 1976), we would be able to detect in a given filter. Using this $L_{\rm lim}$, we can determine the probability of detection of a galaxy, $P_{\rm detect}$, under the simplifying assumption that the likelihood of a galaxy producing an SGRB is proportional to its luminosity.[3] Specifically, $P_{\rm detect}$ describes the fraction of the luminosity-weighted luminosity function that we probe with increasing redshift. To perform this analysis, we used the templates for Sbc, Ell and Irregular (Irr) galaxies from Coleman, Wu & Weedman (1980) and considered magnitudes in the SDSS r' band. We note that the template used is based on an aggregate of observed local galaxies and so includes typical levels of extinction appropriate for the galaxy type. In addition, we have neglected the effect of surface brightness dimming, but we expect this to be a small effect for these sources which are only marginally resolved. For more detailed information on this analysis, we refer the reader to Appendix B.

Fig. 11 shows this analysis using the detection limits determined for all the hostless GRBs in our sample. Looking at the redshift range thought to be typical for SGRBs ($z < 1$) we find for at least six of the bursts we uncover $\sim$85 per cent of the integrated galaxy luminosity for the Irr galaxy type, $\sim$73 per cent Sbc galaxy type and 55 per cent for the Ell galaxy type. In addition, the extremely deep limit placed on GRB 080503 means that even for the Ell galaxy type, we uncover 88 per cent of the integrated galaxy luminosity. This analysis suggests that it is unlikely that the hostless SGRBs are simply cases of faint, but coincident, hosts in the redshift range for $z < 1$, though this case is less strong for Ell galaxies. Higher redshifts, however, up to e.g. $z \sim 4$, are not ruled out by observations of the afterglows or the limits on coincident host galaxies.

Though the majority of SGRBs have been found at redshifts in the range 0.1–0.9, there is some evidence indicating the existence of a higher redshift population. GRB 090426 has the highest confirmed redshift ($z = 2.609$) of a GRB with $T_{90} < 2$ s (Levesque et al. 2010; Thöne et al. 2011). However, there remains considerable discussion as to its nature with its host galaxy, environment and spectral properties being more suggestive of a massive star progenitor than a compact binary merger despite its short duration (Antonelli et al. 2009; Levesque et al. 2010; Xin et al. 2010; Thöne et al. 2011). There is potential evidence for other SGRBs at high redshift with indications for a $z > 4.0$ host for GRB 060121 (de Ugarte Postigo et al. 2006; Levan et al. 2006b), beyond the redshift detection limits we have placed for a fainter galaxy, and the faint, possibly high-redshift hosts of GRB 060313 ($z \lesssim 1.7$) (Schady & Pagani 2006) and GRB 051227 (Berger et al. 2007b). In particular, GRB 070707 ($z < 3.6$), has a very faint coincident host at $R \sim 27$ (Piranomonte et al. 2008). These results may indicate that hostless GRBs are a window on to a higher redshift population. However, some hostless SGRBs have been probed to deep limits, especially GRB 080503 with a limit of $F606W > 28.5$ from *HST* (Perley et al. 2009). If the delay-time distribution for SGRB progenitors is long, then we would expect to preferentially see them at lower redshift. Under the binary neutron star model a significant component will be created around the peak of the Universal star formation rate and so will merge in a time $\sim 10^9$ yr after this era (O'Shaughnessy, Belczynski & Kalogera 2008).

A further constraint on the high-redshift scenario can be obtained simply by contrasting the properties of the long and short host populations. To first order, LGRBs should trace the global star formation rate (allowing for plausible biases introduced by metallicity, which could increase the high-z, low-z rate). In contrast, SGRBs (assuming they have a stellar progenitor), trace the star formation rate convolved with a delay time distribution. In other words, in general we would expect the SGRB redshift distribution to be skewed towards lower redshifts, than for the LGRBs. The samples of Fruchter et al. (2006), Savaglio, Glazebrook & Le Borgne (2009), Svensson et al. (2010), all measured 15–20 per cent of the optically localized LGRB host galaxies have $R > 26.5$. However, the optically unbiased GRB host survey (TOUGH; Hjorth et al. 2012) finds this value to be 30 per cent. This difference is likely due to the differing redshift distributions of LGRBs between *Swift* and previous missions (Jakobsson et al. 2006), with most of the non-detections in the TOUGH sample lying at $z > 3$. To these same limits $\sim$30 per cent of SGRBs are 'hostless'. If the underlying redshift distribution is identical between SGRBs and LGRBs then we cannot draw a strong conclusion either way. However, if SGRBs are a lower redshift population on average then the non-detection of a similar fraction of events to the same limits would seem more surprising.

4.2 The kicked scenario

The possible preference for hostless SGRB sight lines to lie close to bright galaxies, with low $P_{\rm chance}$ relative to random positions on the sky, offers support for models in which we are observing the hostless SGRBs to arise from systems kicked from their hosts at high velocities (several hundred km s^{-1}), and potentially with significant time between their creation and explosion as a GRB ($\sim 10^9$ yr). For the seven secure hostless GRBs in our sample, using $z = 0.3$ where the redshift is unknown, the average offset is $\sim$36 kpc with offsets ranging from $\lesssim 6.6$ to $\sim$85 kpc.

We consider the implications this model would have for hostless SGRBs here.

For the limited sample of (12) SGRBs with optical positions, confidently identified host galaxies and measured redshifts, the physical offsets shown in Table A1 are mostly relatively low (e.g. 051221A, 050724, 070714B), with an overall mean of $\approx$6 kpc. There are some, however, which are further from their host galaxy centres either in the outskirts (e.g. 080905A, 071227) or outside of the host galaxy (e.g. 070429B, 090510). For the hostless SGRBs, physical offsets $>$30 kpc are measured for the suggested host galaxies with confirmed redshifts (e.g. 061201, 070809, 090515; Berger 2010; Fong et al. 2010; Rowlinson et al. 2010b) and $\gtrsim$6 kpc for the cases with only an upper limit on the redshift (e.g. 080503; Perley et al. 2009).

Within the considerable uncertainties, the measured SGRB offset distribution (assuming the galaxy with the lowest $P_{\rm chance}$ is the host in the hostless cases) does appear broadly consistent with predictions for the positions of NS-NS and NS-BH binary mergers using host galaxies of mass comparable to the Milky Way (Fong et al. 2010) and using estimated galaxy masses for the SGRBs (Church et al. 2011). However, in some individual cases, the offsets from the galaxies with the lowest $P_{\rm chance}$ are surprisingly large given these

[3] But see also Belczynski et al. (2006).

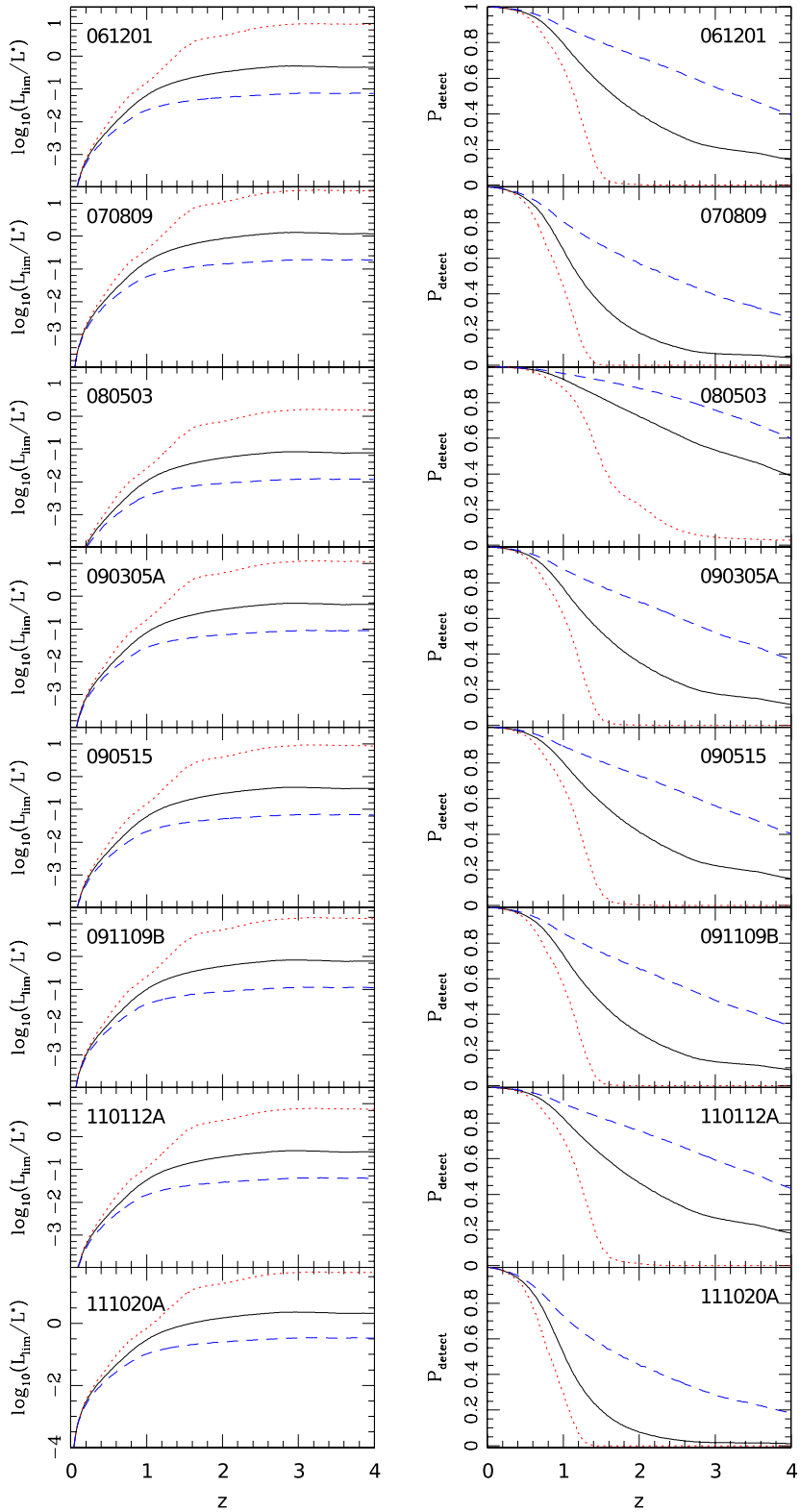

Figure 11. The set of panels on the left-hand side show the minimum luminosity galaxy, $L_{\rm lim}$, we could detect as a function of redshift in the SDSS r' band and based on the magnitude limits of all the hostless GRBs in our sample. Each of these panels contains this evolution for an Sbc (black, solid line), Ell (red, dotted line) and Irr (blue, dashed line) galaxy. We use our measured deepest r' limits placed on GRB 090305A, 091109B (both adapted from the VLT R-band limits) and 110112A (extrapolated from the Gemini-N i' band). We have also included published limits for GRBs 061201, 070809, 080503, 090515 and 111020A (Perley et al. 2009; Berger 2010; Fong et al. 2012) again adapted to the r' band where necessary. There is a deeper limiting magnitude for GRB 111020A from Fong et al. (2011b) and hence this value is used here rather than our reported limit. Note that this includes a simple linear evolution of the luminosity function with further details in Appendix B. Using these $L_{\rm lim}$ values, we then plot the fraction of the integrated luminosity we probe at increasing redshift in the right-hand set of panels ($P_{\rm detect}$). This is again shown for the three types of galaxies we consider here.

predictions, including hostless GRBs 061201, 070809 and XRT-localized 060502B (Church et al. 2011).

Larger offsets would also be a natural product of neutron star binary progenitors formed via a dynamical channel within GCs where a neutron star captures a companion through three-body interactions (Grindlay et al. 2006). For GRBs 061201 and 070809 Salvaterra et al. (2010) suggested that their bright afterglows preclude a location in the IGM and suggested the dynamical channel as the most likely solution. However, SGRBs with optical afterglows have been detected outside their host galaxies, most likely within a low-density medium if not within the IGM, meaning at least in some cases that the afterglow can be detected (Berger 2011) (although it is not possible to rule out the possibility that these bursts also originated from within cluster environments). Indeed, for the hostless GRBs presented here, along with GRB 090515 (Rowlinson et al. 2010b), their faint afterglows could be in line with their being embedded within the IGM, with detection being possible since they are at low redshift.

Another important consideration is that lower mass host galaxies, due to their shallower potential wells and therefore lower escape velocities, should typically exhibit larger burst offsets due to unbound binaries. For dwarf galaxies, we would expect a non-negligible fraction of binary mergers to be found >30 kpc from their host centres (Bloom et al. 2002). Using an evolving galactic potential, the merger sites may be even more diffusively distributed with respect to their host galaxies and may occur out to a few Mpc for lighter haloes (Zemp, Ramirez-Ruiz & Diemand 2009). Particularly given that for dwarf galaxies, even at moderate redshifts ($z \sim 1$), their intrinsic faintness would make them more difficult to detect, this means that it would be more difficult to associate such an SGRB with its low-mass host galaxy and so these cases would appear as being hostless. In this case, it could be that these fainter galaxies are within the halo of a larger galaxy and this is the reason we are seeing a suggested association with larger galaxies at low redshift.

4.3 Implications for co-incident gravitational waves

Perhaps the strongest constraints on the nature of SGRBs will come via searches for simultaneous gravitational wave signals (Phinney 1991; Abadie et al. 2010). For NS-NS binaries such signals should be detectable to next generation GW detectors to distances of ∼500 Mpc NS-NS and ∼1 Gpc NS-BH (Abadie et al. 2010), meaning that SGRBs within this horizon can have sensitive searches for inspirals performed. To date, relatively few of the detected SGRBs fall within this horizon (formally only the lowest $z = 0.105$, GRB 080905A Rowlinson et al. 2010a is consistent with NS-NS or NS-BH detection), suggesting in common with independent analysis (e.g. Abbott et al. 2010) that simultaneous detections with *Swift* and GW detectors will be rare. One possibility which could increase the event rate would be if the hostless SGRBs were in fact kicked from local structures within the horizon of the new advanced detectors. Our observations suggest that in general this is not the case, most of the candidate host galaxies are too faint to lie within this volume, and there are not many bright galaxies within several arcminutes (corresponding to projected distances of several hundred kpc at a distance of 100 Mpc) of the GRB positions.

In the case of GRB 111020A there is an apparently local galaxy with low $P_{\rm chance}$ (equal to the lowest $P_{\rm chance}$ in the field). This galaxy, at an apparent distance of ∼80 Mpc is comfortably within the threshold for GW detection with next generation instrumentation, although in this case the energy release of the burst of $E_{\rm iso} \sim 10^{46}$ ergs would be far lower than typical for SGRBs, while the offset from the host would strongly disfavour events akin to soft-gamma repeaters (Hurley et al. 2005; Tanvir et al. 2005). In addition, for the rest of the hostless SGRB sample, we searched the NASA extragalactic database (NED)[4] (Schmitz et al. 2011) for any bright, low-redshift host within 10 arcmin of the GRB position. Galaxy 2MASX J13350593−2206302 (also designated 6dFGS gJ133506.0−220631 in the 6dFGS catalogue) is detected within 50 arcsec of GRB 070809 with magnitude $R = 15.38$ (Jones et al. 2004, 2009). With redshift $z = 0.042\,783$ (Paturel et al. 2003) this galaxy is within 190 Mpc, again within the GW detection volume. These situations are rather similar to the more poorly constrained case of GRB 050906 (Levan & Tanvir 2005) whose γ-ray only position places it close on the sky to IC 328, and whose energy (if associated with IC 328) would be similar. Nonetheless, such associations on the sky are rare; of the ∼700 LGRBs detected by *Swift* to date, only ∼3 contain bright ($R < 15$) low-redshift galaxies within a few arcminutes of the burst position that ultimately turned out not to be associated with the burst. This supports the conclusions shown in Fig. 9.

These results suggest that we should expect to see a handful of SGRBs within the GW horizon per year (all sky), but also imply that the hostless SGRBs likely contribute no more to this population than those with optically identified hosts.

5 CONCLUSIONS

We have looked at the afterglow properties of three apparently hostless SGRBs: GRB 090305A, GRB 091109B and GRB 111020A. The former, in particular, had a very faint X-ray counterpart, only identified due to the detection of the optical afterglow within the BAT error circle. Detection of the afterglow of GRB 091109B in the R band and GRB 090305A in the g' band allows us to place upper redshift limits of $z \lesssim 5$ and $z \lesssim 3.5$, respectively.

Deep optical observations at the GRB position after the afterglow had faded allows us to put constraints on any coincident host galaxy, specifically the 3σ limiting magnitude for GRB 090305A is $r > 25.69$, for GRB 091109B the limits are $R > 25.80$, $K > 22.23$ and $J > 21.99$ and for GRB 111020A is $R > 24.23$ (a deeper limit of $i' > 24.4$ has also been placed by Fong et al. 2012). Although r'-band observations make Ell galaxies in particular difficult to detect with lower redshift limits, use of a deep limit in the K band would even the chances of detecting any type of host galaxy. Using the deepest limiting magnitudes for GRBs 090305A and 091109B, we find that out to $z = 1$ we uncover ∼75 per cent of the integrated galaxy luminosity for an Sbc-type galaxy, ∼85 per cent for an Irr galaxy and 55 per cent for an Ell galaxy. GRB 111020A which, even using the deepest limit available from Fong et al. 2012, has a shallower limit, would uncover ∼50 per cent (Sbc galaxy). It is unclear as to the status of GRB 111020A as a hostless burst due to the presence of an unresolved object 0.7 arcsec from its position which would have $P_{\rm chance} < 0.01$.[5] However, for other GRBs considered here as well as no coincident host detection, we also find no host that can be confidently identified using $P_{\rm chance}$ values (<1 per cent).

These GRBs represent a growing population of optically localized SGRBs with no obvious host galaxy. We have considered two possible origins for these hostless SGRBs. The first is that they

[4] http://ned.ipac.caltech.edu/

[5] This case is also complicated by the relatively low Galactic latitude, which means that foreground stars significantly outnumber background galaxies in our images.

originate from a higher redshift, and so far unseen population of SGRBs, while the second is that they lie at lower redshift, and are kicked from local, and relatively bright host galaxies.

To address these issues, we developed a diagnostic to assess the significance of the association of any given galaxies with an SGRB, and compared the properties of the sample of bursts with those of random positions on the sky. These results suggest that hostless SGRBs as a population have a correlation with structure at small angular scales, more so that 'average' random lines of sight. This perhaps offers evidence that the hostless SGRBs are in fact associated either with these bright galaxies, or with fainter galaxies associated with the same large-scale structure. In this case, the offsets are either as a result of large-scale natal kicks to the progenitors, or of their dynamical formation within GCs.

We note that a similar study by Berger (2010) concluded that large offsets of 15–70 kpc from relatively low-redshift galaxies are their preferred explanation. They found for a high-redshift solution the constraints on any underlying host galaxy implied a bimodal population of SGRBs with peaks at $z \sim 0.5$ and $z \sim 3$. They also allow for a minor contribution from NS binary mergers in GCs. Our work broadly agrees with the results considered by Berger (2010), although critically extends it to consider the true distribution of galaxies on the sky (rather than average number of counts), utilizing this comparison to make statistical statements on the population as a whole.

Ultimately, if hostless GRBs are present at low redshift, deeper observations of their locations will continue to yield null detections of their host galaxies. However, for bursts associated with structure at lower redshift we may be able to ascertain if they are hosted within GCs via deep observations with either the *HST* (to $z < 0.1$) or the James Webb Space Telescope (to $z < 0.2$). Such a detection could offer strong evidence for the origin of SGRBs in compact binary mergers.

ACKNOWLEDGEMENTS

We thank Edo Berger and Wen-fai Fong for discussion, and the provision of the Gemini imaging of GRB 110112A. RLT thanks STFC for a studentship award. AJL, NRT, KW acknowledge receipt of STFC funding via rolling grant awards. Based on observations made with ESO Telescopes at the La Silla Paranal Observatory under programme IDs 088.D-0523, 084.D-0621, 082.D-0451. Based on observations obtained at the Gemini Observatory, which is operated by the Association of Universities for Research in Astronomy, Inc., under a cooperative agreement with the NSF on behalf of the Gemini partnership: the National Science Foundation (United States), the Science and Technology Facilities Council (United Kingdom), the National Research Council (Canada), CONICYT (Chile), the Australian Research Council (Australia), Ministério da Ciência, Tecnologia e Inovação (Brazil) and Ministerio de Ciencia, Tecnología e Innovación Productiva (Argentina). These observations are associated with programmes GN-2009A-Q-23 and GN-2011A-Q-4. The DARK cosmology centre is funded by the DNRF.

REFERENCES

Abadie J. et al., 2010, Classical Quantum Gravity, 27, 173001
Abazajian K. N. et al., 2009, ApJS, 182, 543
Abbott B. P. et al., 2010, ApJ, 715, 1438
Antonelli L. A. et al., 2009, A&A, 507, L45
Barthelmy S. D. et al., 2005a, Space Sci. Rev., 120, 143
Barthelmy S. et al., 2005b, GCN Circ., 3385, 1
Barthelmy S. D. et al., 2009, GCN Circ., 9364, 1
Barthelmy S. D., Sakamoto T., Stamatikos M., 2011, GCN Circ., 11557, 1
Beardmore A. P., Cummings J. R., Holland S. T., Markwardt C. B., Pagani C., Page K. L., Palmer D. M., 2009a, GCN Circ., 8932, 1
Beardmore A. P., Page K. L., Evans P. A., Pagani C., Kennea J., Burrows D. N., 2009b, GCN Circ., 8937, 1
Belczynski K., Perna R., Bulik T., Kalogera V., Ivanova N., Lamb D. Q., 2006, ApJ, 648, 1110
Berger E., 2009, ApJ, 690, 231
Berger E., 2010, ApJ, 722, 1946
Berger E., 2011, New Astron. Rev., 55, 1
Berger E. et al., 2005, Nature, 438, 988
Berger E., Shin M.-S., Mulchaey J. S., Jeltema T. E., 2007a, ApJ, 660, 496
Berger E. et al., 2007b, ApJ, 664, 1000
Berger E., Cenko S. B., Fox D. B., Cucchiara A., 2009, ApJ, 704, 877
Berger E., Chornock R., Cucchiara A., Fox D. B., 2010, GCN Circ., 10346, 1
Berger E., Fong W., Chornock R., 2013, ApJ, 774, L23
Bloom J. S., Prochaska J. X., 2006, in Holt S. S., Gehrels N., Nousek J. A., eds, AIP Conf. Ser. Vol. 836, Gamma-Ray Bursts in the Swift Era. Am. Inst. Phys., New York, p. 473
Bloom J. S., Sigurdsson S., Pols O. R., 1999, MNRAS, 305, 763
Bloom J. S., Kulkarni S. R., Djorgovski S. G., 2002, AJ, 123, 1111
Bloom J. S. et al., 2006, ApJ, 638, 354
Bloom J. S. et al., 2007, ApJ, 654, 878
Bromberg O., Nakar E., Piran T., Sari R., 2013, ApJ, 764, 179
Burrows D. N. et al., 2005, Space Sci. Rev., 120, 165
Cannizzo J. K. et al., 2006, GCN Rep., 20, 1
Capak P. et al., 2007, ApJS, 172, 99
Cenko S. B. et al., 2008, preprint (arXiv:0802.0874)
Cenko S. B., Cobb B. E., Perley D. A., Bloom J. S., 2009, GCN Circ., 8933, 1
Cenko S. B., Levan A. J., Chornock R., Berger E., Perley D. A., Bloom J. S., Tanvir N., 2010, GCN Circ., 11468, 1
Chornock R., Fong W., Berger E., Persson E., 2010, GCN Circ., 11469, 1
Church R. P., Levan A. J., Davies M. B., Tanvir N., 2011, MNRAS, 413, 2004
Coleman G. D., Wu C., Weedman D. W., 1980, ApJS, 43, 393
Cucchiara A., Cenko S. B., 2011, GCN Circ., 12567, 1
Cummings J. et al., 2005, GCN Circ., 4365, 1
Curran P. A., Beardmore A. P., Page K. L., Krimm H. A., Barthelmy S. D., Marshall F. E., 2009, GCN Rep., 224.1
D'Avanzo P. et al., 2009, A&A, 498, 711
De Pasquale M., Markwardt C., Sbarufatti B., 2010, GCN Rep., 269.1
de Ugarte Postigo A. et al., 2006, ApJ, 648, L83
Donaghy T. Q. et al., 2006, preprint (arXiv:0605570)
Eichler D., Livio M., Piran T., Schramm D. N., 1989, Nature, 340, 126
Evans P. A. et al., 2007, A&A, 469, 379
Evans P. A., Goad M. R., Osborne J. P., Beardmore A. P., 2009, GCN Circ., 151, 1
Fong W., Berger E., 2011, GCN Circ., 12470, 1
Fong W., Berger E., Fox D. B., 2010, ApJ, 708, 9
Fong W. et al., 2011a, ApJ, 730, 26
Fong W., Berger E., Fox D., 2011b, GCN Circ., 12467, 1
Fong W. et al., 2012, ApJ, 756, 189
Fong W. et al., 2013, ApJ, 769, 56
Fruchter A. S. et al., 2006, Nature, 441, 463
Fryer C. L., Woosley S. E., Hartmann D. H., 1999, ApJ, 526, 152
Galeev A. et al., 2009, GCN Circ., 9549, 1
Gehrels N. et al., 2005, Nature, 437, 851
Golenetskii S. et al., 2011, GCN Circ., 12715, 1
Grindlay J., Portegies Zwart S., McMillan S., 2006, Nat. Phys., 2, 116
Guidorzi C. et al., 2007, GCN Rep., 77.1
Hjorth J., Bloom J. S., 2011, in Kouveliotou C., Wijers R. A. M. J., Woosley S., eds, Cambridge Astrophysics Series, Vol. 51: The Gamma-Ray Burst – Supernova Connection. Cambridge Univ. Press, Cambridge, p. 169
Hjorth J. et al., 2005, Nature, 437, 859

Hjorth J. et al., 2012, ApJ, 756, 187
Holland S. T., Landsman W. B., Page K. L., Stamatikos M., 2010, GCN Rep., 289.1
Hook I. M., Jørgensen I., Allington-Smith J. R., Davies R. L., Metcalfe N., Murowinski R. G., Crampton D., 2004, PASP, 116, 425
Hoversten E. A., Krimm H. A., Grupe D., Kuin N. P. M., Barthelmy S. D., Burrows D. N., Roming P., Gehrels N., 2009, GCN Rep, 218.1
Hullinger D. et al., 2005, GCN Circ., 4400, 1
Hurley K. et al., 2005, Nature, 434, 1098
Ilbert O. et al., 2005, A&A, 439, 863
Jakobsson P. et al., 2006, A&A, 447, 897
Jakobsson P., Hjorth J., Malesani D., Fynbo J. P. U., Krühler T., Milvang-Jensen B., Tanvir N. R., 2012, in Peter W. A. R., Nobuyuki K., Elena P., eds, Proc. IAU Symp. 279, The Death of Massive Stars: Supernovae and Gamma-Ray Bursts. Cambridge Univ. Press, Cambridge, p. 187
Jones D. H. et al., 2004, MNRAS, 355, 747
Jones D. H. et al., 2009, MNRAS, 399, 683
Kann D. A. et al., 2011, ApJ, 734, 96
Kocevski D. et al., 2010, MNRAS, 404, 963
Kraft R. P., Burrows D. N., Nousek J. A., 1991, ApJ, 374, 344
Krimm H. et al., 2005, GCN Circ., 3667, 1
Krimm H. A. et al., 2008, GCN Circ., 8735, 1
Krimm H. A. et al., 2009, GCN Circ., 8936, 1
Krimm H. A., Cummings J. R., Evans P. A., Marshall F. E., 2010a, GCN Rep., 271, 1
Krimm H. A. et al., 2010b, GCN Circ., 11467, 1
Krimm H. A., Landsman W., Marshall F. E., Pagani C., 2011, GCN Rep., 312, 1
Levan A., Tanvir N., 2005, GCN Circ., 3927, 1
Levan A. J., Tanvir N. R., 2010, GCN Circ., 10887, 1
Levan A. J., Wynn G. A., Chapman R., Davies M. B., King A. R., Priddey R. S., Tanvir N. R., 2006a, MNRAS, 368, L1
Levan A. J. et al., 2006b, ApJ, 648, L9
Levan A. J. et al., 2007, MNRAS, 378, 1439
Levan A. J. et al., 2008, MNRAS, 384, 541
Levan A. J., Tanvir N. R., Hjorth J., Malesani D., de Ugarte Postigo A., D'Avanzo P., 2009, GCN Circ., 10154, 1
Levan A. J., Tanvir N. R., Baker D., 2011, GCN Circ., 11559, 1
Levesque E. M. et al., 2010, MNRAS, 401, 963
Malesani D., de Ugarte Postigo A., Levan A. J., Tanvir N. R., Hjorth J., D'Avanzo P., 2009, GCN Circ., 10156, 1
Mangano V., Baumgartner W. H., Mangano V., Immler S., Barthelmy S. D., Burrows D. N., Siegel M. H., Gehrels N., 2012, GCN Rep., 363.1
Mao J., Guidorzi C., Ukwatta T., Brown P. J., Barthelmy S. D., Burrows D. N., Roming P., Gehrels N., 2008, GCN Rep., 138.1
Margutti R. et al., 2012, ApJ, 756, 63
Markwardt C. et al., 2006, GCN Circ., 4873, 1
Markwardt C., Beardmore A., Marshall F. E., Schady P., Barthelmy S. D., Burrows D. N., Roming P., Gehrels N., 2007, GCN Rep., 51.1
Marshall F. E., Perri M., Stratta G., Barthelmy S. D., Krimm H., Burrows D. N., Roming P., Gehrels N., 2006, GCN Rep., 18.1
Marshall F. E., Barthelmy S. D., Burrows D. N., Chester M. M., Cummings J., Evans P. A., Roming P., Gehrels N., 2007, GCN Rep., 80.1
McBreen S. et al., 2010, A&A, 516, A71
McGlynn S., Foley S., McBreen S., Hanlon L., O'Connor R., Carrillo A. M., McBreen B., 2008, A&A, 486, 405
Metzger B. D., Thompson T. A., Quataert E., 2007, ApJ, 659, 561
Miller A. A., Perley D. A., Bloom J. S., Cenko S. B., Nugent P. E., 2010, GCN Circ., 10377, 1
Montero-Dorta A. D., Prada F., 2009, MNRAS, 399, 1106
Nicuesa Guelbenzu A. et al., 2012, A&A, 548, A101
Nugent P. E., Bloom J. S., 2010, GCN Circ., 11491, 1
O'Shaughnessy R., Belczynski K., Kalogera V., 2008, ApJ, 675, 566
Oates S. R. et al., 2009a, GCN Circ., 148, 1
Oates S. R., Page K. L., Evans P. A., Markwardt C. B., 2009b, GCN Rep., 259.1
Ohno M., McEnery J., Pelassa V., 2009, GCN Circ., 168, 1
Pagani C., Racusin J. L., Brown P., Cummings J., 2008, GCN Rep., 162.1
Paturel G., Petit C., Rousseau J., Vauglin I., 2003, A&A, 405, 1
Perley D. A., Bloom J. S., Modjaz M., Poznanski D., Thoene C. C., 2007, GCN Circ., 7140, 1
Perley D. A., Bloom J. S., Modjaz M., Miller A. A., Shiode J., Brewer J., Starr D., Kennedy R., 2008, GCN Circ., 7889, 1
Perley D. A. et al., 2009, ApJ, 696, 1871
Perley D. A., Berger E., Cenko S. B., Chornock R., Levan A. J., Tanvir N., 2010, GCN Circ., 11464, 1
Phinney E. S., 1991, ApJ, 380, L17
Piranomonte S. et al., 2008, A&A, 491, 183
Prochaska J. X., Bloom J. S., Chen H.-W., Hansen B., Kalirai J., Rich M., Richer H., 2005, GCN Circ., 3700, 1
Prochaska J. X. et al., 2006, ApJ, 642, 989
Racusin J., Barbier L., Landsman W., 2007, GCN Rep., 70.1
Rau A., McBreen S., Kruehler T., 2009, GCN Circ., 9353, 1
Rowlinson A. et al., 2010a, MNRAS, 408, 383
Rowlinson A. et al., 2010b, MNRAS, 409, 531
Sakamoto T. et al., 2011a, GCN Circ., 12464, 1
Sakamoto T. et al., 2011b, GCN Circ., 12460, 1
Salvaterra R., Cerutti A., Chincarini G., Colpi M., Guidorzi C., Romano P., 2008, MNRAS, 388, L6
Salvaterra R., Devecchi B., Colpi M., D'Avanzo P., 2010, MNRAS, 406, 1248
Sari R., Piran T., Narayan R., 1998, ApJ, 497, L17
Sato G. et al., 2005a, GCN Circ., 3793, 1
Sato G. et al., 2005b, GCN Circ., 4318, 1
Sato G. et al., 2006a, GCN Circ., 5064, 1
Sato G. et al., 2006b, GCN Circ., 5381, 1
Sato G. et al., 2007, GCN Circ., 7148, 1
Sato G. et al., 2009, GCN Circ., 9263, 1
Savaglio S., Glazebrook K., Le Borgne D., 2009, ApJ, 691, 182
Schady P., Pagani C., 2006, GCN Circ., 4877, 1
Schady P. et al., 2006, GCN Rep., 6.1
Schechter P., 1976, ApJ, 203, 297
Schlegel D. J., Finkbeiner D. P., Davis M., 1998, ApJ, 500, 525
Schmitz M. et al., 2011, Am. Astron. Soc., 217, 344.08
Siegel M. H., Grupe D., 2011, GCN Circ., 12717, 1
Soderberg A. M. et al., 2006, ApJ, 650, 261
Stamatikos M. et al., 2011, GCN Circ., 11553, 1
Stratta G. et al., 2007, A&A, 474, 827
Svensson K. M., Levan A. J., Tanvir N. R., Fruchter A. S., Strolger L.-G., 2010, MNRAS, 405, 57
Tanvir N. R., Levan A. J., 2010, GCN Circ., 10905, 1
Tanvir N. R., Chapman R., Levan A. J., Priddey R. S., 2005, Nature, 438, 991
Tanvir N. R. et al., 2012, ApJ, 754, 46
Tanvir N. R., Levan A. J., Fruchter A. S., Hjorth J., Hounsell R. A., Wiersema K., Tunnicliffe R. L., 2013, Nature, 500, 547
Thöne C. C. et al., 2011, MNRAS, 414, 479
Troja E., King A. R., O'Brien P. T., Lyons N., Cusumano G., 2008, MNRAS, 385, L10
Villasenor J. S. et al., 2005, Nature, 437, 855
Wong T., Willems B., Kalogera V., 2010, ApJ, 721, 1689
Xin L. et al., 2010, MNRAS, 401, 2005
Xin L. P., Zhang T. M., Qiu Y. L., Wei J. Y., Wang J., Deng J. S., Wu C., Han X. H., 2011, GCN Circ., 11554, 1
Xu D., Ilyin I., Fynbo J. P. U., 2010, GCN Circ., 11492, 1
Zemp M., Ramirez-Ruiz E., Diemand J., 2009, ApJ, 705, L186
Ziaeepour H. et al., 2007a, GCN Rep., 21.2
Ziaeepour H. et al., 2007b, GCN Rep., 74.2

APPENDIX A: SGRB SAMPLE

The putative host galaxies of the optically localized SGRB sample considered in this paper are detailed in Table A1. This SGRB sample has been subdivided into those with small and large offsets. To do this, we use the methodology of Fruchter et al. (2006) to calculate

Table A1. Host galaxy details for all well-localized SGRBs up to 2012 April (25 GRBs). The designation of on-host, off-host is described in the main text. The host galaxy listed is the one with the lowest $P_{\rm chance}$ value.

GRB	T_{90}[a] (s)	Fluence[a] (10^{-7} erg cm^{-2})	$F_{\rm light}$	Host mag (r'(AB))[b]	z	Offset (arcsec)	Offset (kpc)	Ref.
				On-host GRBs				
SGRBs								
051221A	1.40 ± 0.20	11.6 ± 0.4	0.54–0.65	21.99 ± 0.09	0.55	0.12 ± 0.04	0.76 ± 0.25	[1]–[3]
060121	1.97 ± 0.06[c]	38.7 ± 2.7[c]		26.2 ± 0.3	>4.0	0.119 ± 0.046	–	[4]–[7]
070429B	0.50 ± 0.10	0.63 ± 0.10		23.18 ± 0.10	0.9023	0.6	4.7	[8]–[10]
070707	0.8 ± 0.2[d]	$2.07^{+0.06}_{-0.32}$[d]		27.66 ± 0.13[e]	<3.6	0.1 ± 0.3	–	[11]–[12]
070724A	0.40 ± 0.04	0.30 ± 0.07	0.19	20.56 ± 0.03	0.46	0.71 ± 2.1	4 ± 12	[3], [13], [14]
071227	1.80 ± 0.00	2.2 ± 0.3	0.19	20.66[f]	0.38	2.9 ± 0.4	15.0 ± 2.2	[3], [15], [16]
081226A	0.4 ± 0.1	0.99 ± 0.18		25.79 ± 0.34		<0.5		[17], [18]
090426	1.20 ± 0.30	1.8 ± 0.3		24.47 ± 0.15[g]	2.6	0.1	0.8	[19]–[21]
100117A	0.30 ± 0.05	0.93 ± 0.13		24.33 ± 0.10	0.92	0.6	–	[22], [23]
111117A	0.47 ± 0.09	1.40 ± 0.18		23.6	$1.3^{+0.3}_{-0.2}$	1.25 ± 0.20	10.5 ± 1.7	[24]–[26]
EE GRBs								
050709	0.07 ± 0.01[c]	3.03 ± 0.38[c]		21.46 ± 0.2[f]	0.1606	1.33	3.64	[7], [27]–[29]
050724	3 ± 1	6.3 ± 1.0	0.03–0.33	18.36 ± 0.03[f]	0.258	0.64 ± 0.02	2.57 ± 0.08	[28], [30]–[32]
051227	8 ± 2	2.3 ± 0.3	0.66	$25.78^{0.18}_{0.12}$		0.05 ± 0.02	<0.7	[16], [33], [34]
061006	130 ± 10	14.3 ± 1.4	0.56–0.63	24.18 ± 0.09	0.436	0.3 ± 0.3	3.5	[16], [34], [35]
070714B	64 ± 5	7.2 ± 0.9	0.26	25.39 ± 0.23[f]	0.9225	0.4	3.1	[10], [36]
				Off-host GRBs				
SGRBs								
060313	0.70 ± 0.1	11.3 ± 0.5	0.00–0.04	25.16 ± 0.20[e]		0.4	–	[34], [37]
080905A	1.00 ± 0.10	1.4 ± 0.2	0.00	18.4 ± 0.5[f]	0.122	9	18.5	[38], [39]
090510	0.30 ± 0.10	3.4 ± 0.4	0.00	23.4 ± 0.07	0.9	1.2	9.4	[40]–[42]
				Hostless SGRBs				
SGRBs								
061201	0.80 ± 0.10	3.3 ± 0.3	–	18.09[h]	0.111	16.2	32.4	[7], [43], [44]
070809	1.30 ± 0.10	1.0 ± 0.1	–	21.8 ± 0.3[f]	0.473	6.0	35.4	[45]–[47]
090305A	0.4 ± 0.1	0.75 ± 0.13	–	25.64 ± 0.20		1.5	–	[48]
090515	0.04 ± 0.02	0.2 ± 0.08	–	20.2 ± 0.1	0.403	14	75.2	[47], [49], [50]
091109B	0.27 ± 0.05	1.9 ± 0.2	–	23.88 ± 0.1[e]		3.0	–	[51]
110112A	0.5 ± 0.1	0.30 ± 0.09	–	21.42 ± 0.13		19.3	–	[52]
111020A	0.40 ± 0.09	0.65 ± 0.10	–	23.336 ± 0.10		3.0	–	[53], [54]
EE GRBs								
080503	170 ± 40	20 ± 1	–	27.19 ± 0.2[i]	<4	0.8	<6.6	[47], [55], [56]

[a] T_{90} and Fluence are given in the 15–150 keV energy band unless otherwise stated. [b] All magnitudes in this table are in the AB magnitude system and have values corrected for Galactic absorption (Schlegel et al. 1998). Where we do not know the galaxy magnitude in the r' band a colour correction is made from the magnitude in the closest filter using the most appropriate of the four standard SED templates (Sbc, Scd, Ell, Im) from Coleman et al. (1980) and the galaxy redshift where known. When the galaxy type is not known the Sbc template is used. [c] *HETE-2* trigger. T_{90} and Fluence of GRB 060121 are given in the 30–400 keV energy band. [d] *INTEGRAL* trigger. T_{90} and Fluence of GRB 070707 are given in the 20–200 keV energy band. [e] For GRBs 070707, 060313 and 091109B no redshift for the most likely host galaxy is available. R-band magnitudes for these galaxies are converted to r' band using the Sbc template at $z = 1$. [f] R-band magnitude of the host galaxies of GRBs 071227, 050709, 050724, 070714B, 080905A, 070809 have been converted using the known redshift and an appropriate galaxy type. [g] We convert the V band of the host galaxy of GRB 090426 to the r' band using the Irr galaxy template. [h] $F606W$ band magnitude of the host galaxy of GRB 061201 with the lowest $P_{\rm chance}$ has been converted to the r' band using known redshift and the Sbc galaxy type. [i] i' band magnitude of the galaxy with the lowest $P_{\rm chance}$ for GRB 110112A has been converted using $z = 0$ and the Sbc galaxy template. [j] J-band magnitude of the galaxy with lowest $P_{\rm chance}$ for GRB 111020A has been converted to the r' band using $z = 0$ and the Sbc galaxy type. [k] $F606W$ band magnitude of the galaxy of GRB 080503 with the lowest $P_{\rm chance}$ has been converted to the r' band using $z = 1$ and the Sbc galaxy type.

References: [1] Cummings et al. (2005), [2] Soderberg et al. (2006), [3] Berger (2009), [4] Donaghy et al. (2006), [5] Levan et al. (2006b), [6] de Ugarte Postigo et al. (2006), [7] Fong et al. (2010), [8] Markwardt et al. (2007), [9] Perley et al. (2007), [10] Cenko et al. (2008), [11] McGlynn et al. (2008), [12] Piranomonte et al. (2008), [13] Ziaeepour et al. (2007b), [14] Berger et al. (2009), [15] Sato et al. (2007), [16] D'Avanzo et al. (2009), [17] Krimm et al. (2008), [18] Nicuesa Guelbenzu et al. (2012), [19] Sato et al. (2009), [20] Levesque et al. (2010), [21] Antonelli et al. (2009), [22] De Pasquale, Markwardt & Sbarufatti (2010), [23] Fong et al. (2011a), [24] Mangano et al. (2012), [25] Margutti et al. (2012), [26] Cucchiara & Cenko (2011), [27] Villasenor et al. (2005), [28] Troja et al. (2008), [29] Prochaska et al. (2006), [30] Krimm et al. (2005), [31] Prochaska et al. (2005), [32] Berger et al. (2005), [33] Hullinger et al. (2005), [34] Berger et al. (2007b), [35] Schady et al. (2006), [36] Racusin, Barbier & Landsman (2007), [37] Markwardt et al. (2006), [38] Pagani et al. (2008), [39] Rowlinson et al. (2010a), [40], Hoversten et al. (2009), [41] Rau, McBreen & Kruehler (2009), [42] McBreen et al. (2010), [43] Marshall et al. (2006), [44] Stratta et al. (2007), [45] Marshall et al. (2007), [46] Perley et al. (2008), [47] Berger (2010), [48] Krimm et al. (2009), [49] Barthelmy et al. (2009), [50] Rowlinson et al. (2010b), [51] Oates et al. (2009b), [52] Barthelmy et al. (2011), [53] Sakamoto et al. (2011a), [54] Fong et al. (2012), [55] Mao et al. (2008), [56] Perley et al. (2009).

Table A2. Host galaxy details, where available, for XRT-localized SGRBs up to 2012 April (16 GRBs). The host galaxy listed is the one with the lowest $P_{\rm chance}$ value.

GRB	T_{90}[a] (s)	Fluence[a] (10^{-7} erg cm^{-2})	Host mag (r'(AB))[b]	z	Offset (arcsec)	Offset (kpc)	X-ray error radius (arcsec)	Ref.
SGRBs								
050509B	0.13	0.23 ± 0.09	17.18 ± 0.05[c]	0.2248	17.7	63.4	3.4	[1]–[4]
050813	0.6 ± 0.1	1.24 ± 0.46	24.18 ± 0.07[c]	0.719	4.9	35.5	2.9	[5], [6]
051210	1.27 ± 0.05	0.83 ± 0.14	23.80 ± 0.15	$\gtrsim$1.4	2.9	>24.9	2.9	[7], [8]
060502B	0.09 ± 0.02	0.4 ± 0.05	19.17 ± 0.01[c]	0.287	17.1	73.3	4.36	[9], [10]
060801	0.5 ± 0.1	0.81 ± 0.10	23.20 ± 0.11	1.1304	2.1	17.6	1.5	[8], [11]
061217	0.212 ± 0.041	0.46 ± 0.8	23.33 ± 0.07	0.827	1.9	14.4	1.89	[8], [12]
070729	0.9 ± 0.1	1.0 ± 0.2	23.77 ± 0.25[d]		10.0	–	2.5	[4], [13]
090621B	0.14 ± 0.04	0.70 ± 0.10	21.83 ± 0.11[d]		11.5	–	5.1	[14], [15]
100206A	0.12 ± 0.03	1.4 ± 0.2	21.3 ± 0.3[d]		3.7	–	2.1	[16], [17]
100625A	0.33 ± 0.03	2.3 ± 0.2	$\sim$23		0.5	–	1.8	[18]–[20]
101219A	0.6 ± 0.2	4.6 ± 0.3	$\sim$24.4[e]	0.718	0.5	3.5	2.4	[21]–[24]
101224A	0.2 ± 0.01	0.58 ± 0.11	20.8 ± 0.2[f]		$\sim$0.5	–	3.2	[25]–[27]
111222A	0.32[g]	72 ± 7[g]	18.08 ± 0.01		0.48	–	2.9	[28], [29]
EE GRBs								
061210	85 ± 5	11 ± 2	21.00 ± 0.02	0.4095	2.9	15.6	1.8	[8], [30]

[a]As for Table A1, T_{90} and Fluence are given in the 15–150 keV energy band unless otherwise stated. [b]As for Table A1 all magnitudes in this table are in the AB magnitude system and have values corrected for Galactic absorption (Schlegel et al. 1998). Where we do not know the galaxy magnitude in the r' band a colour correction is made from the magnitude in the closest filter using the most appropriate of the four standard SED templates (Sbc, Scd, Ell, Im) from Coleman et al. (1980) and the galaxy redshift where known. When the galaxy type is not known the Sbc template is used. [c]*R*-band magnitude of the host galaxies of GRBs 050509B, 050813, 060502B have been converted using the known redshift and the Ell galaxy type. [d]For GRBs 070729, 090621B and 100206A no redshift for the most likely host galaxy is available. *R*-band magnitudes for these galaxies are converted to r' band using the Sbc template at $z = 1$. [e]The i' magnitude for the host of GRB 101219A has been converted to the r' band using the Sbc template at $z = 0.718$. [f]*V*-band magnitude of the most likely host galaxy of GRB 101224A has been converted using the Sbc template at $z = 1$. [g]*INTEGRAL* trigger. T_{90} and Fluence of GRB 111222A are given in the 20−30 MeV energy band and were measured by the *Konus–Wind* instrument.

References: [1] Barthelmy et al. (2005b), [2] Bloom et al. (2006), [3] Fong et al. (2010), [4] Berger (2009), [5] Sato et al. (2005a), [6] Prochaska et al. (2006), [7] Sato et al. (2005b), [8] Berger et al. (2007b), [9] Sato et al. (2006a), [10] Bloom et al. (2007), [11] Sato et al. (2006b), [12] Ziaeepour et al. (2007a), [13] Guidorzi et al. (2007), [14] Curran et al. (2009), [15] Galeev et al. (2009), [16] Krimm et al. (2010a), [17] Miller et al. (2010), [18] Holland et al. (2010), [19] Levan & Tanvir (2010), [20] Tanvir & Levan (2010), [21] Krimm et al. (2010b), [22] Chornock et al. (2010), [23] Cenko et al. (2010), [24] Perley et al. (2010), [25] Krimm et al. (2011), [26] Nugent & Bloom (2010), [27] Xu, Ilyin & Fynbo (2010), [28] Golenetskii et al. (2011), [29] Siegel & Grupe (2011), [30] Cannizzo et al. (2006).

$F_{\rm light}$ which is the fraction of total galaxy light in regions of lower surface brightness than at the position of the GRB. Any burst with $F_{\rm light} > 0$ must be within the host and $F_{\rm light} = 0$ indicates it is not. We use values of $F_{\rm light}$ from Fong et al. (2010), supplementing these with our own values based on our VLT imaging of GRB 080905A and GRB 090510. In the few cases, when no $F_{\rm light}$ measurement is available, we assume the GRBs are on the light of their hosts, especially since these GRBs are at low offsets. Where possible we have also considered a sample of SGRBs which only have XRT-localizations with the host galaxy details listed in Table A2.

APPENDIX B: DETERMINATION OF $P_{\rm detect}$

To perform the analysis described in Section 4.1, we used an evolving galaxy luminosity function represented by a Schechter function (Schechter 1976) where the number density of galaxies per unit luminosity, $\phi(L)$, is given by equation (B1).

$$\phi(L)\mathrm{d}L = \phi^* \left(\frac{L}{L^*}\right)^{\alpha} \exp\left(-\frac{L}{L^*}\right) \frac{\mathrm{d}L}{L^*}, \tag{B1}$$

where L^* parameterizes the position of the knee in the luminosity function. For typical values of α, the bulk of the integrated luminosity is contributed by galaxies around L^*. For increasing redshift, we use a simple linear evolution of the luminosity function, investigating the magnitudes in the SDSS r' band up to $z = 4$. We use a value of $M_r^* = -21.48$ at $z = 0$ from Montero-Dorta & Prada (2009) and an adapted value for $M_r^* = -22.88$ at $z = 2.0$ from Ilbert et al. (2005), using $r'(AB) = R(AB) + 0.06$ (Sbc), $= R(AB) + 0.06$ (Ell) and $= R(AB) + 0.04$ (Irr) appropriate for the galaxy templates used (Coleman et al. 1980). Similarly we also evolved α from $\alpha_{z=0} = -1.26$ at $z = 0$ (Montero-Dorta & Prada 2009) to $\alpha_{z=2} = -1.53$ at $z = 2$ (Ilbert et al. 2005). The minimum galaxy luminosity detectable with our detection limits, $L_{\rm lim}$, is determined using the PYTHON ASTSED module as part of the ASTLIB package. The probability of detection, $P_{\rm detect}$, as function of redshift can be determined using equation (B2).

$$P_{\rm detect} = \int_{L_{\rm low}}^{L_{\rm lim}} L\phi(L)\mathrm{d}L \Big/ \int_{L_{\rm low}}^{\infty} L\phi(L)\mathrm{d}L, \tag{B2}$$

where we define $M_{\rm low} = -10$ as the magnitude corresponding to a suitable lower limit on galaxy luminosities. To first order, we assume that the SGRB rate is proportional to the host galaxy luminosity. Our chosen cosmology was $\Omega_{\rm M} = 0.3$, $\Omega_\lambda = 0.7$ and $H_0 = 70\,\mathrm{km\,s^{-1}\,Mpc^{-1}}$.

This paper has been typeset from a TEX/LATEX file prepared by the author.